AD-A134 792 SEA SALT AEROSOL ATMOSPHERIC RADON AND METEOROLOGICAL OBSERVATIONS IN THE..(U) NAVAL RESEARCH LAB WASHINGTON DC F K LEPPLE ET AL. 28 SEP 83 NRL-MR-5153 1/1

UNCLASSIFIED F/G 8/10 NL

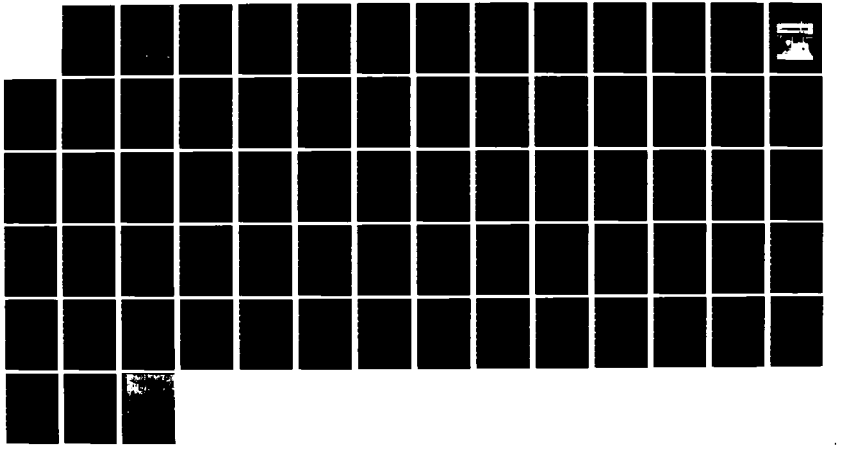

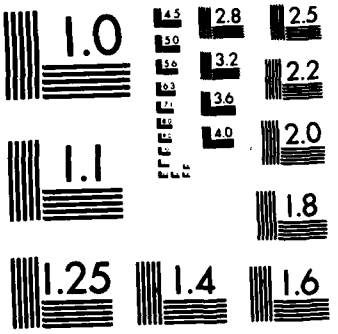

NRL Memorandum Report 5153

Sea Salt Aerosol, Atmospheric Radon and Meteorological Observations in the Western South Atlantic Ocean (February 1981)

F. K. LEPPLE, D. J. BRESSAN AND J. B HOOVER

Environmental Chemistry Branch
Environmental Sciences Division

R. E. LARSON

Atmospheric Physics Branch
Environmental Sciences Division

September 28, 1983

NAVAL RESEARCH LABORATORY
Washington, D.C.

SECURITY CLASSIFICATION OF THIS PAGE (When Data Entered)

REPORT DOCUMENTATION PAGE	READ INSTRUCTIONS BEFORE COMPLETING FORM
1. REPORT NUMBER: NRL Memorandum Report 5153 — 2. GOVT ACCESSION NO.: AD-A134	3. RECIPIENT'S CATALOG NUMBER: 742
4. TITLE (and Subtitle): SEA SALT AEROSOL, ATMOSPHERIC RADON AND METEOROLOGICAL OBSERVATIONS IN THE WESTERN SOUTH ATLANTIC OCEAN (FEBRUARY 1981)	5. TYPE OF REPORT & PERIOD COVERED: Interim report on a continuing NRL problem.
	6. PERFORMING ORG. REPORT NUMBER
7. AUTHOR(s): F.K. Lepple, D.J. Bressan, J.B. Hoover and R.E. Larson	8. CONTRACT OR GRANT NUMBER(s)
9. PERFORMING ORGANIZATION NAME AND ADDRESS: Naval Research Laboratory, Washington, DC 20375	10. PROGRAM ELEMENT, PROJECT, TASK AREA & WORK UNIT NUMBERS: 43-1130-0-3
11. CONTROLLING OFFICE NAME AND ADDRESS	12. REPORT DATE: September 28, 1983
	13. NUMBER OF PAGES: 69
14. MONITORING AGENCY NAME & ADDRESS(if different from Controlling Office)	15. SECURITY CLASS. (of this report): UNCLASSIFIED
	15a. DECLASSIFICATION/DOWNGRADING SCHEDULE

16. DISTRIBUTION STATEMENT (of this Report)

Approved for public release; distribution unlimited.

17. DISTRIBUTION STATEMENT (of the abstract entered in Block 20, if different from Report)

18. SUPPLEMENTARY NOTES

19. KEY WORDS (Continue on reverse side if necessary and identify by block number)

Sea salt aerosol
Marine aerosol concentrations
Atmospheric radon measurements
Boundary layer meteorology

20. ABSTRACT (Continue on reverse side if necessary and identify by block number)

The concentration of sea salt aerosol was measured aboard the USNS HAYES at 16m height in the western South Atlantic Ocean from Februar, 3-19, 1981. Aerosol samples were collected using a NRL-designed, automated sampler coupled to a programmable environmental monitoring system. Simultaneous measurements of wind speed and direction, air and water temperature, relative humidity, barometric pressure and atmospheric radon concentration were also made nearly continuously along the cruise track. Emphasis on functional relationships between synoptic measurements of sea salt

(Continues)

DD FORM 1 JAN 73 1473 EDITION OF 1 NOV 65 IS OBSOLETE
S/N 0102-014-6601

SECURITY CLASSIFICATION OF THIS PAGE (When Data Entered)

20. ABSTRACT (Continued)

aerosol and local wind speed showed the overall correlation between these two parameters to be poor ($r \leq 0.3$ for 249 data point sets). However, when the data is separated into discrete meteorological and/or oceanographic events, most short term correlations are significantly improved.

In this region of the South Atlantic Ocean, we attribute the low overall correlation between synoptic measurements of salt aerosol and wind speed to the effects of hysteresis, condensation processes and varying structure of the turbulent boundary layer. The sea surface temperature varied widely during this cruise and seemed to directly influence the atmospheric salt load, regardless of wind speed in many cases. Deterministic predictions of instantaneous sea salt aerosol values will require improved real-time methods for characterizing the marine boundary layer.

Alternatively, modelling sea salt aerosol concentrations might be most practically effected using a statistical approach. Removing the temporal constraints by ordering the salt aerosol and wind speed data sets results in an extremely high ($r = 0.99$) correlation coefficient. This gives promise for the estimation of sea salt aerosol distributions from wind speed distributions for specific oceanic areas and seasons.

CONTENTS

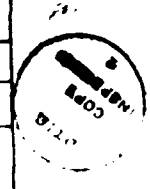

List of Figures and Captions

List of Tables

SEA SALT AEROSOL, ATMOSPHERIC RADON AND METEOROLOGICAL OBSERVATIONS IN THE WESTERN SOUTH ATLANTIC OCEAN (FEBRUARY 1981)

BACKGROUND

Several naval systems require reliable sea salt aerosol models for predicting atmospheric optical propagation, understanding precipitation and fog formation, and for protecting materials on ships and aircraft operating in the marine environment. The continuous cycling of sea salt between the ocean and atmosphere often involves several geochemical processes such as enrichments of heavy metals, (Piotrowicz et al., 1979), nutrients (Graham et al., 1979) and organic material (Barger and Garrett, 1970) in sea salt particles transferred to the atmosphere. However, an initial step in developing global climatological pictures of sea salt aerosols is identification and evaluation of relationships between measurable properties of sea salt aerosols and various meteorological parameters. Wind stress on the ocean surface is currently of special interest as a generator of bubbles which later burst, producing both jet and film droplets. This mechanism is thought by Wu (1981) to be the major producer of salt aerosol. Several investigators (Woodcock, 1953; Toba, 1961; Tsunogai et al., 1972; Savoie and Prospero, 1977 and Lovett, 1978) have studied the relationship between local wind speed and sea salt aerosol concentration. Lovett's (1978) study in the North Atlantic was a most extensive work (more than 1800 samples over an 11-month period) and it shows that the mathematical relationship between a given wind speed and the measured atmospheric sea salt aerosol concentration can vary by as much as a factor of ten.

The situation, however, is more complicated than indicated above. As noted in the literature, sea salt aerosol concentrations should be affected by the previous wind conditions and air mass histories, thus requiring both advective and local determinants of concentration. Characteristics of the local air mass and surface features of the sea are also expected to influence the production of sea salt aerosols. Relevant parameters would presumably include air temperature and relative humidity, atmospheric turbulence and mixing height, air mass time over the ocean, wind fetch, sea surface water temperature, local wave patterns and surface films. Much remains to be done in these parametric areas to account for probable

Manuscript approved July 20, 1983.

geographical differences. Most investigations to date have attempted to relate the generation of sea salt aerosol to local wind speed. Two important aspects of these previous investigations may have obscured important features of the relationships: first, nearly all of the data was collected at wind speeds less than 12 m/sec and secondly, the wind and sea salt aerosol concentration data was averaged over relatively long time periods (4 to 24 hours).

During February 1981, we had an opportunity to sample the marine aerosol nearly continuously for 16 days during an oceanographic cruise in the western South Atlantic Ocean. In light of the foregoing remarks, our goal was to measure and record the short-term variability of sea salt aerosol concentrations on time scales of less than 2 hours between samples. We then attempted to correlate measured sea salt aerosol concentrations with wind speed and other relevant parameters.

EXPERIMENTAL

Samples of marine aerosols, atmospheric radon data and meteorological information were taken nearly continuously along the cruise track of the USNS HAYES both while underway and on oceanographic stations. The cruise track, station numbers and number designation of the aerosol samples collected underway are displayed in Figure 1. Station locations, arrival and departure times are listed in Table 1.

An unattended device, the ARCAS I (for Automatic Radon Counter and Aerosol Sampler) was used to collect one set of aerosol samples. This instrument also counted the radon daughter product decay and printed a nearly real-time record for each sample (see Bressan, 1981 for complete details of operation). ARCAS I consists of a deck-mounted sampling unit and an indoor electronic unit containing controls, calendar clock with display, thumbwheels for manual data entry and a thermal printer. Figure 2 illustrates the aerosol sampling unit mounted forward on the flying bridge at the mid-line of the USNS HAYES. The inlet height is approximately 16 m above sea level. Wind tunnel tests showed nearly horizontal air flow in this region which has unobstructed trajectories ± 120° from straight ahead. For this cruise, the ARCAS was set to sample air for 20 minutes every 90 minutes and then count the decay of radioactive radon daughter products for nine ten-minute intervals. The 5-cm-diameter samples are sequentially taken and stored on a incremented roll of glass fiber filter

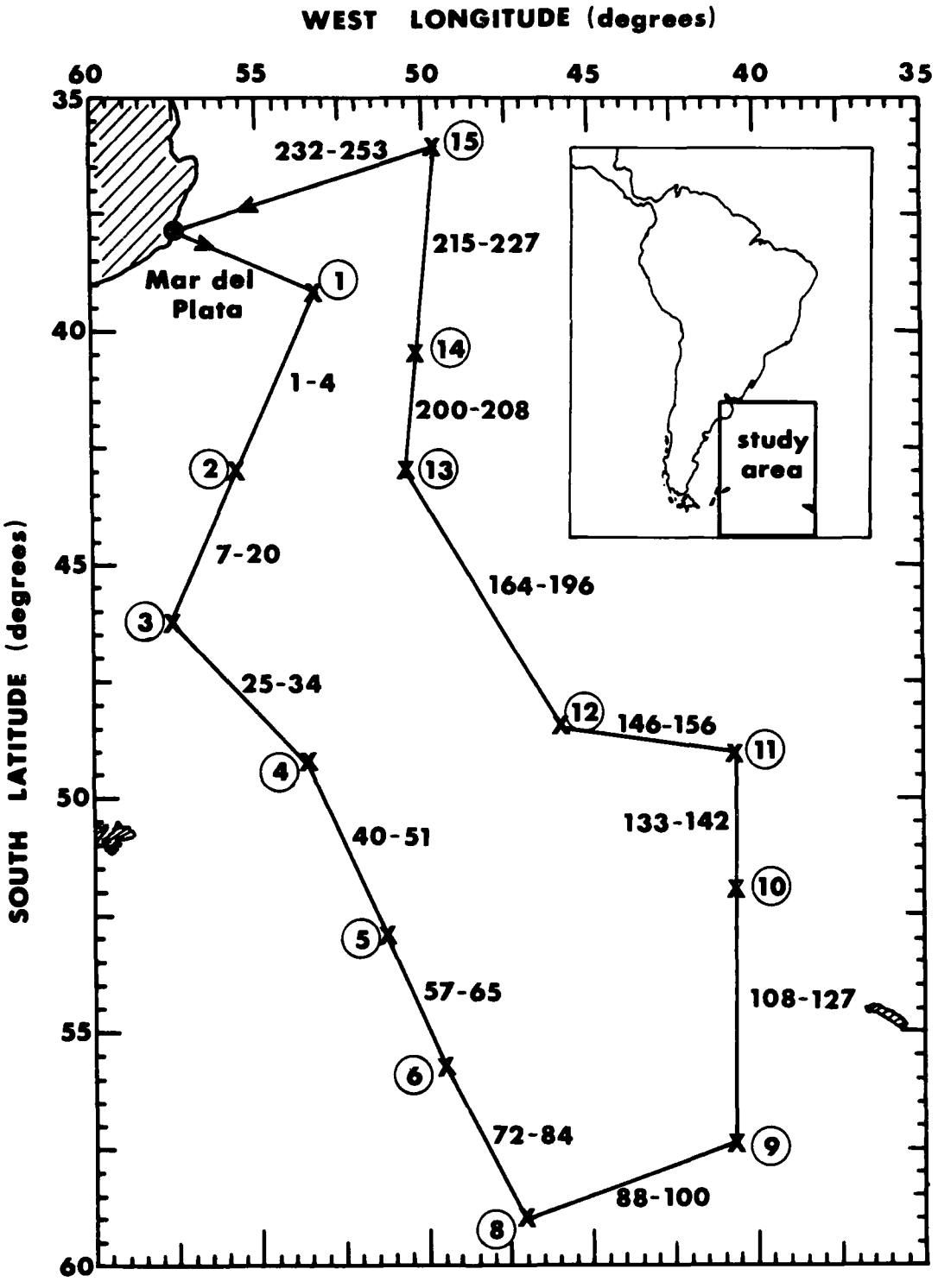

Fig. 1 — Track of USNS HAYES (Cruise 81-16-02) leaving Mar del Plata, Argentina on February 1 and returning February 19, 1981. Circled numbers refer to oceanographic stations while numbers along cruise track designate aerosol samples collected underway.

Table 1 — Oceanographic station positions, arrival and departure times

Station	Position Lat.(S) Long.(W)	Arrive JD	Arrive GMT	Depart JD	Depart GMT
Mar del Plata	37°55', 57°30'	--	--	032	2000
1	39°12', 53°17'	033	1240	034	0225
2	43°04', 55°36'	034	2000	034	2300
3	46°19', 57°37'	035	2120	036	0125
4	49°19', 53°30'	036	2035	037	0040
5	53°01', 51°11'	037	1920	038	0140
6	55°47', 49°25'	038	1615	039	0110
8	59°01', 47°00'	039	2010	040	0000
9	57°25', 40°41'	040	2020	041	0710
10	52°00', 40°40'	042	1515	042	2115
11	49°00', 40°40'	043	1115	043	1720
12	48°31', 45°49'	044	1030	044	2000
13	42°59', 50°33'	046	2100	047	0230
14	40°31', 50°14'	047	1530	048	0010
15	36°05', 49°38'	048	2100	049	0125
Mar del Plata	37°55', 57°30'	050	0900	--	--

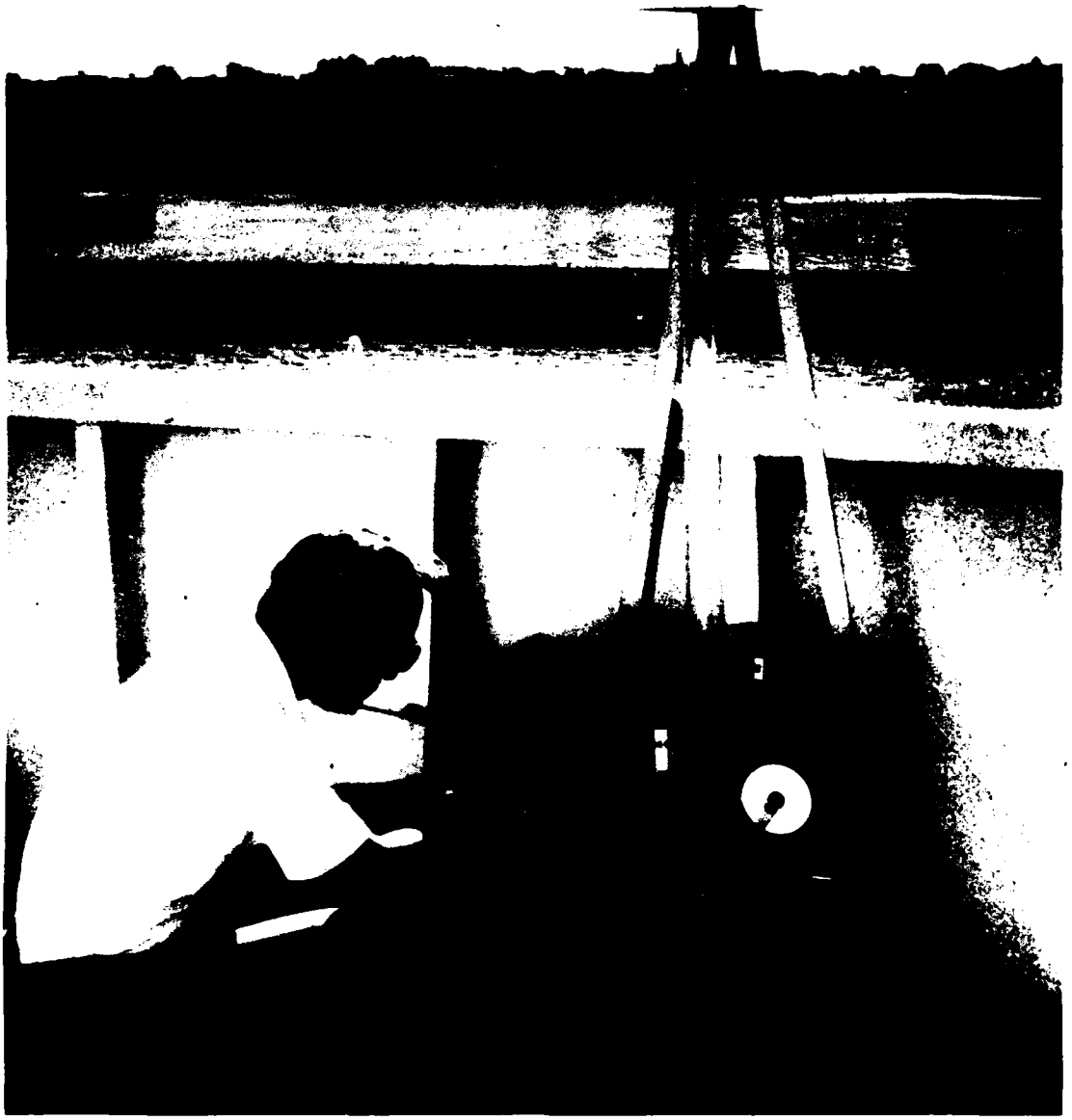

79941

Fig. 2 — Photograph of automated aerosol sampler and radon counter (ARCAS I) mounted on flying bridge of USNS HAYES.

paper (Hollingsworth and Vose HE 1022). After each sample passes between a pair of radiation counting tubes (Larson and Bressan, 1978), it is covered with a layer of mylar film. This prevents sample cross-contamination as the aerosol samples are rolled onto the filter paper takeup spool. The air flow rate was 1.33 m^3/min, yielding a sample volume of approximately 27 m^3 of air for each aerosol collection.

The air inlet shown in Figure 2 was designed to keep out rain and large fog or spray drops, yet allow smaller droplets and sea salt particles to enter from any direction. Estimations of the most likely air flow patterns with computations (after Hochrainer, 1978) of viscous drag forces indicate that for wind speeds up to 31 m/sec (60 knots), salt particles up to at least 40 μm diameter should follow the air flow pattern down the inlet tube, while particles of 100 μm diameter would certainly impact on the opposite inner wall of the vertical inlet tube above this wind speed. Biasing against extremely large droplet sizes will minimize collection of any spray generated by ship motion.

The beta-radioactive daughter products of radon-222 collected on the filter paper roll were detected with a thin plastic scintillator mounted on a photomultiplier tube (Larson, 1973). The radon counting electronics were calibrated before and after the cruise using Tc^{99} as a beta source. The lower limit of detection for this device is approximately 0.2 pCi/m^3 with an absolute uncertainty of ± 15% over the range of concentrations encountered in this study.

At NRL, the aerosol samples were individually cut from the filter tape roll and extracted on a 47 mm Millipore filter holder with 200 ml of distilled deionized water maintained at 50° - 60°C. The leachates were analyzed for sodium content by flame atomic absorption using a Perkin-Elmer Model 373 spectrophotometer. The soluble sodium was assumed to be derived only from sea salt. Estimates of total sea salt in each sample are obtained by multiplying the sodium value by 3.25, which is the salinity to sodium ratio in bulk seawater (Riley and Chester, 1971). The sodium content of the 5-cm-diameter glass fiber filter blanks averaged 18 μg ± 12% (n=20 samples). Based on an average sample volume of 27 m^3, the background "salt" level produced by the sodium blank in each filter would be equivalent to 2.2 $\mu g/m^3$.

A specially designed high-volume (hi-vol) air sampler (Lepple, 1975) was also operated on the HAYES to collect marine aerosols over a longer time interval (7-18 hours each). This hi-vol, which is constructed of polyvinyl chloride, has one 2.5 cm x 25 cm inlet slit which can be manually adjusted to obtain approximately isokinetic sampling conditions. The blower motor for the hi-vol was separated from the filter holder unit by a one-meter length of flexible hose to minimize possible aerosol contamination from the carbon brushes and the motor armature. The hi-vol was mounted on the forward edge of the flying bridge bulkhead about 15 m above sea level and within 3 meters of the ARCAS inlet. The flow rate through the 20 cm x 25 cm glass fiber filters was approximately 1.7 m^3/minute. For these HV filters, the sea salt component was measured by extracting the soluble sodium in one-half of the filter using the same technique as for the ARCAS samples.

The NRL Environmental Monitoring System (EMS) was used to obtain meteorological information at 15-minute intervals and provide outputs to both printed paper tape and magnetic tape. The system consists of a Fluke Model 2240B data logger, a Columbia Data Products Model 300C Data Cartridge Recorder and several sensors and signal conditioners. Measurements included relative wind speed and direction (Teledyne Geotech Model 201), relative humidity (General Eastern Model 450), barometric pressure (Texas Electronics Model 2012), and ambient temperature (General Eastern and Fluke platinum resistance probes). The temperature and relative humidity sensors were mounted in a Climet aspirated shield (Model 016-2) which was located on the rear mast of the HAYES approximately 21 m above sea level. Estimated accuracy of the meteorological sensors is as follows: wind speed: ± 0.5m/sec or 2% of true air speed, whichever is greater; threshold velocity 1 m/sec; wind direction: ± 3°; relative humidity: ± 3% between 15% and 99% R. H. ; temperature: ± 0.5°C for General Eastern PRT, ± 0.2°C for Fluke PRT: and barometric pressure: ± 1% from set point of 760 torr.

Ship speed and heading were entered manually into the EMS to provide data for computer calculation of true wind speed and direction. Power supply voltages for the system sensors were also routinely monitored to help screen for potentially bad or missing data.

Radon decay counts and EMS data were processed at the laboratory on a DEC-10 computer using the METEOR FORTRAN programs, which were developed at NRL (Hoover, 1982).

Unfortunately, many of the wind measurements being fed into the data logger were compromised due to interference from the ship's electrical system. Thus, instead of having automated wind data 4 times per hour as planned, we had to rely on the data manually recorded in the ship's log every 2 hours. Relative wind was read from the ship's anemometers (at 26 m height), then converted to true wind values by the ship's officers. From our past experience, the accuracy of their data is approximately ± 1.5 m/sec and ± 5°.

RESULTS AND DISCUSSION

Graphs of the sea salt aerosol concentration and local wind speed as a function of time are presented in Figures 3, 4 and 5. More data details such as time of collection, individual and average values of salt concentration, wind speed, and temperature (sea and air) are listed in Table A in the Appendix. The salt aerosol concentrations have been corrected for the sodium blank and have been adjusted to standard conditions (25° C and 760 torr). Also contained in the Appendix are graphs of the surface wave heights, ambient temperature, barometric pressure, relative humidity, atmospheric water vapor and atmospheric radon concentration measured along the cruise track. The radon data and relevant meteorological information are presented first to provide a framework for later interpretation of the sea salt aerosol data.

A) Atmospheric Radon

Radon (^{222}Rn) measurements provide a simple, reliable, real-time indicator of the relative maritime or continental nature of the air over coastal or oceanic areas (Wilkniss, et al., 1974). ^{222}Rn has a half-life of 3.8 days and originates from the decay of ^{226}Ra, a member of the ^{238}U decay chain. At least 98% of ^{222}Rn originates from land masses (Wilkening and Clements, 1975). The radon flux at the surface is dependent upon the radium content of the soils and rocks, the permeability of the source materials, atmospheric pressure, soil moisture and vegetative cover (Larson and Bressan, 1980). Radon concentrations measured a few meters above the surface in North America (Larson and Hoppel, 1973) are of the order of 100 picoCuries per cubic meter. From this source strength, decay to a few pCi/m^3 or less of radon is usually indicative of maritime air which has had a long trajectory over the ocean. Relatively abrupt changes in radon concentration usually indicate changes in air masses and the passage of frontal systems. Radon measurements are especially useful in remote ocean areas where surface meteorological observations are extremely sparse.

The atmospheric radon concentrations measured along the cruise track are plotted in Figure A-7. It is apparent from this time series that the character of the boundary layer air being sampled was frequently changing between being predominantly marine or predominantly continental in

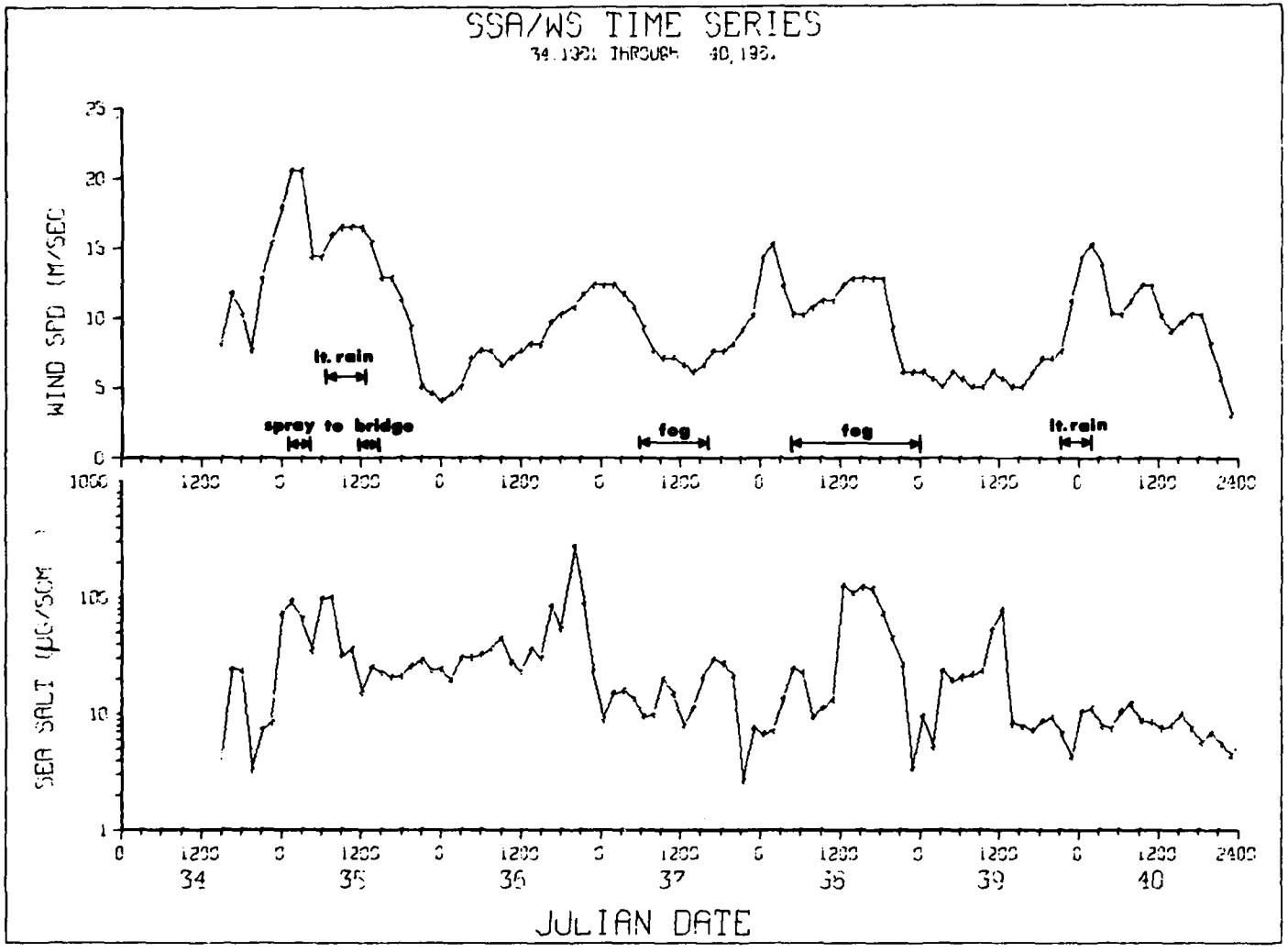

Fig. 3 — Time series plot of sea salt aerosol concentration and local wind speed from JD 34 through JD 40, 1981.

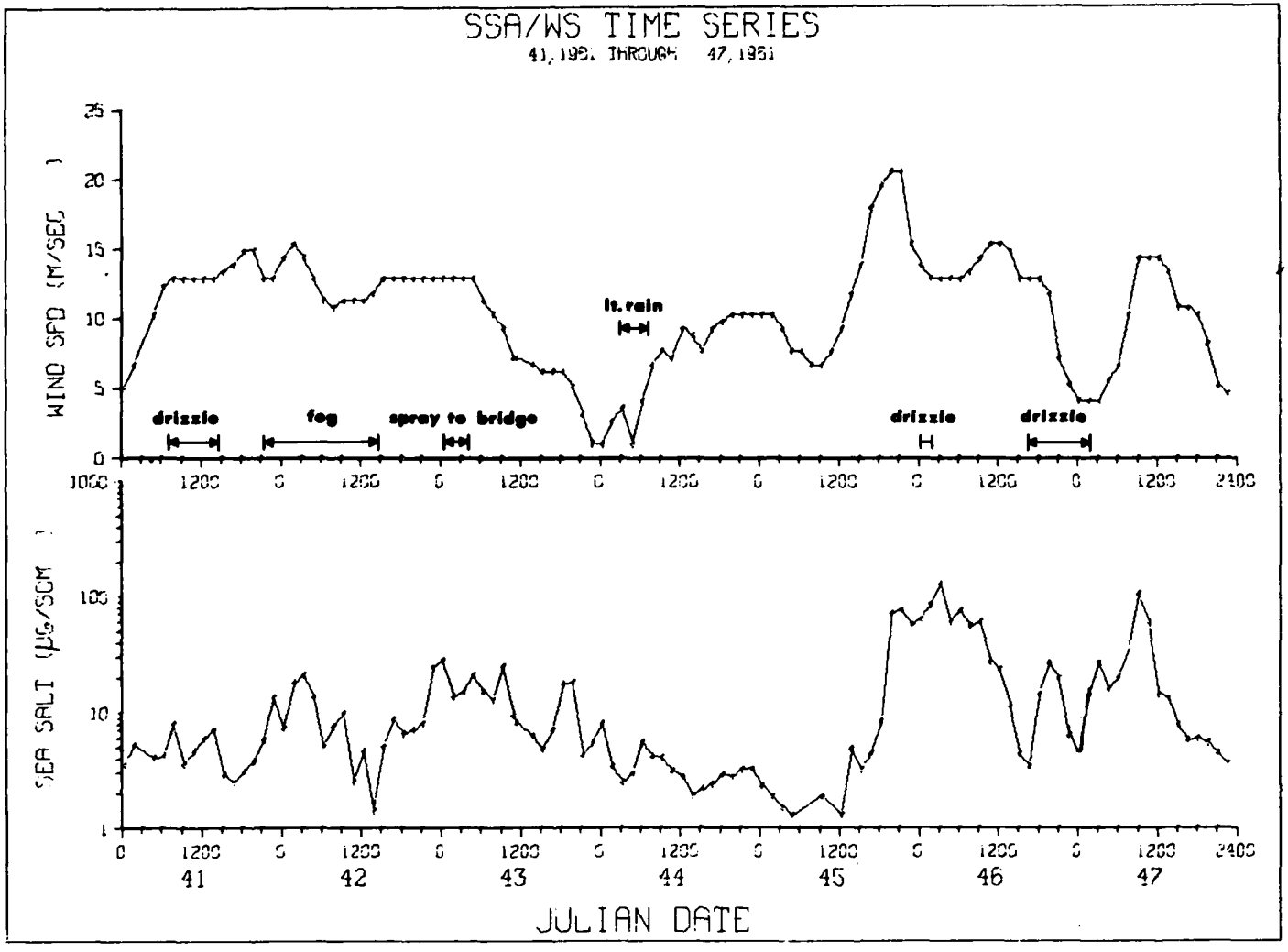

Fig. 4 — Time series plot of sea salt aerosol concentration and local wind speed from JD 41 through JD 47, 1981.

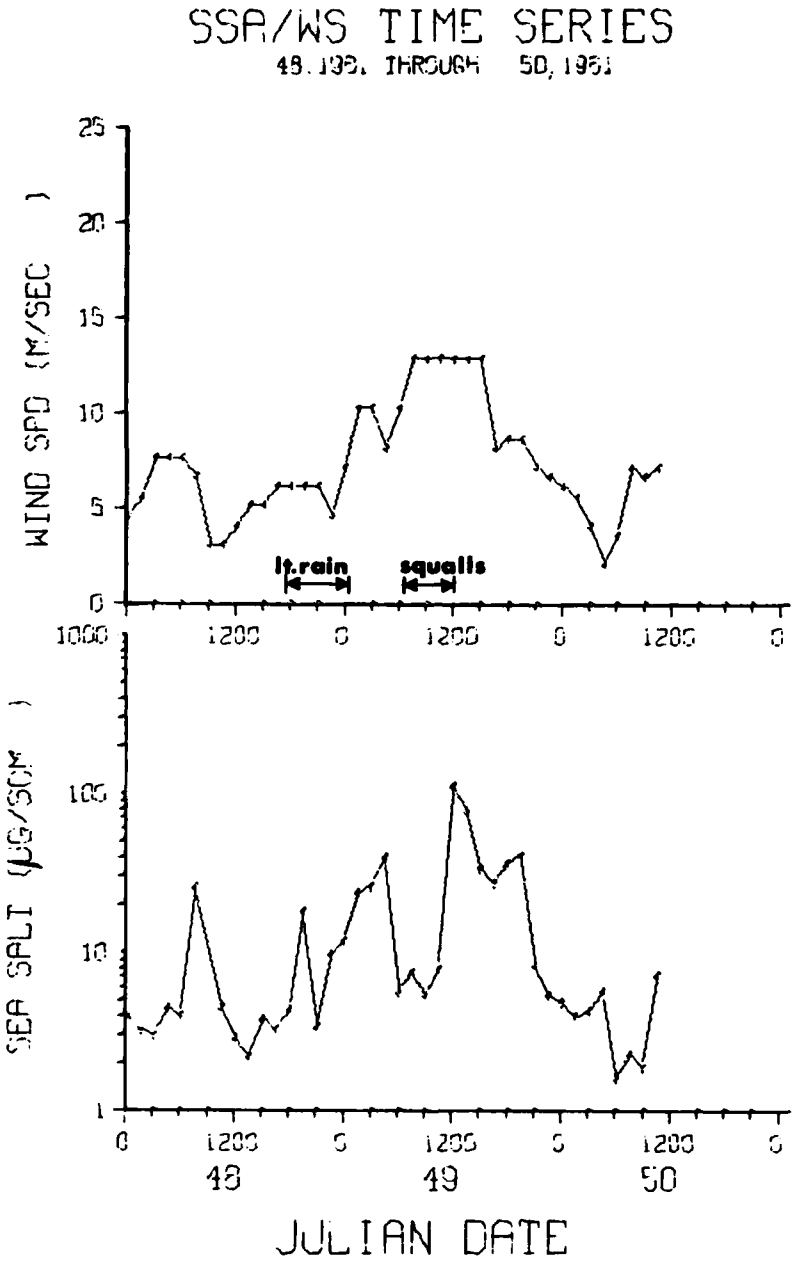

Fig. 5 — Time series plot of sea salt aerosol concentration and local wind speed from JD 48 through JD 50, 1981.

nature. This is illustrated by low or undetectable radon levels in the first case and by peaks to 1 or 2 pCi/m^3 in the second case.

Radon measurements by Lockhart (1960) in southern South America and the radon measurement taken at Mar del Plata (sample 253) suggest that near surface (approx. 15m) radon concentrations over the areas of southern South America may be 15 to 30 pCi/m^3. (This is almost an order of magnitude less than typical continental concentrations found in the Northern Hemisphere). The levels of radon measured hundreds of km offshore during this cruise are reasonable, however, based on this source strength of 15-30 pCi/m^3 and expected intervening mixing processes (Guedalia et al., 1972). A similar case was observed by Wilkniss et al. (1974) in the Southwest Pacific. There, the radon in maritime air was a few tenths of a pCi/m^3 while continental air off Australia showed a few Ci/m^3 of radon.

For this cruise, we obtained streamfunction charts from the National Weather Service to augment our shipboard meteorological observations. These streamfunction (wind flow) charts are derived from computer analysis of satellite data depicting low cloud motions. To aid in the interpretation of the salt aerosol data, radon data is also needed since the streamfunction analyses do not show frontal systems.

The general circulation features derived from a combination of shipboard measurements, streamfunction analyses and radon concentration are presented in the Appendix.

B) Salt Aerosol Observations

The average salt aerosol concentration for the entire cruise was 21.7 ± 30.9 $\mu g/m^3$ (arithmetic mean and standard deviation for 253 samples from the ARCAS). Prospero (1979) has also measured salt aerosol concentrations from ships in the South Atlantic Ocean (at an elevation of 15 m). His overall statistics for 35 samples taken in the tropical and central South Atlantic (5° S to 35° S) are 9.1 ± 5.3 $\mu g/m^3$. When he includes 5 additional samples collected near the Cape of Good Hope, these values become 11.3 ± 9.2 $\mu g/m^3$. A larger salt aerosol concentration is expected in our more southerly sampling region (35° S to 60° S), due to higher average wind speeds there.

Hi-Vol Data

The results of the eight hi-vol aerosol experiments are shown in Table 2 which lists the starting and ending dates and times, and the salt aerosol concentration in units of micrograms per standard cubic meter (all volumes have been adjusted to standard temperature and pressure; designated by SCM). Representative wind speeds and predominant weather conditions are also noted. The color of the exposed filters can be used as a rough indicator of either ship contamination or representative ambient particulate matter in the atmosphere. Except for HV samples 1, 4 and 5, the filters appeared as white as a clean blank filter. This indicates clean local sampling conditions (supported by the presence of relative winds ± 90° from the bow during sampling) and an unpolluted atmosphere. By contrast, aerosol sampling in the North Atlantic usually results in sooty grey or black filters from industrialized continental source areas or heavily traveled shipping lanes (Parkin et. al., 1970; Lepple et. al., 1980). The mild contamination of HV samples 1, 4 and 5 (light grey for HV 1 and HV 5; medium grey for HV 4) can be traced to varying amounts of unfavorable relative wind trajectories over the ship. Lower estimates of salt aerosol concentration are given for HV samples 2 and 6 due to nonlinear changes in the sampling flow rate as the filters became saturated with fog water.

Before proceeding to an examination of the salt aerosol and wind speed time series, it would be instructive to compare empirically the aerosol particle capture characteristics of the hi-vol sampler and ARCAS I. Table 3 lists all the instances where comparisons could be made between these samplers. Note that over the continuous hi-vol sampling period, the ARCAS is sampling 22% of the total time period (20 minutes out of every 90 minutes). For HV samples 4 and 5 when the wind would be expected to produce salt particles less than 60 μm diameter at 98% R. H. (Blanchard and Woodcock, 1980), the mass ratios are in acceptable agreement. For HV sample intervals 7 and 8, obtained during conditions of ship spray and light drizzle, comparison shows that much of the salt is contained in droplets larger then those accepted by the ARCAS inlet.

Comparisons and Data Scatter

Overall, the sea salt aerosol concentrations (Figs. 3-5) show

Table 2 — Hi-vol aerosol sample data

Sample #	Start JD	Start GMT	End JD	End GMT	Salt Aerosol Conc. (μg/SCM)	Wind, Weather
HV 1	32	2215	33	1245	14.6	6-12 m/sec; cloudy
HV 2	34	0243	34	1150	43.	4-3 m/sec; fog
HV 3	34	1250	34	2000	166.7	6-13 m/sec; lt. rain
HV 4	36	0255	36	2105	31.0	7-10 m/sec; clear
HV 5	39	0210	39	2005	45.0	5-8 m/sec; cloudy
HV 6	41	0807	42	1030	170.	10-15 m/sec; heavy fog
HV 7	42	2125	43	1140	295.6	10-13 m/sec; spray on flying bridge
HV 8	43	2010	44	0950	114.9	0-7 m/sec; lt. drizzle

Table 3 — Comparison between hi-vol and ARCAS I aerosol data

Salt Aerosol Conc.

HV #	ARCAS #'s	(μg/SCM) HV	ARCAS I	Ratio HV/ARCAS
4	25-37	45	62	0.7
5	73-84	32	23	1.4
7	132-142	297	16	19
8	148-156	115	5	23

considerable variation with time, but the response to increasing or decreasing local wind speed (also shown in Figs. 3-5) is not always consistent. The fine structure we observe in our data is not evident in the extensive data set plotted in Lovett's thesis, (1975) because his sampling frequency was approximately 4 times per day while ours was 16 times per day. Both data sets show instances when salt aerosol levels either do not change with increasing wind speed or show rapid increases with decreasing wind speed. This exemplifies some of the vagaries encountered which can lead to low point-by-point correlations between wind speed and salt aerosol concentration. The relative attenuation of fine structure in our wind data is due to the low frequency of observation (every 2 hours vs. every hour for Lovett (1975). However, this factor should not unduly affect the data interpretations which follow.

Time Series Intervals

Early in the cruise (day 34 from 1500 to day 38 at 2200, designated Interval 1) and towards the end (day 45 at 0900 to day 50 at 1200, designated Interval 3), the local wind speed and the sea salt aerosol data generally exhibit the same trends with peaks usually coincident in time.

In the middle portion of the cruise (2200 on day 38 to 0900 day 45, designated Interval 2), the salt aerosol concentration apparently shows much less response to the local wind. Except for the salt peak centered around 0800 on day 39, salt concentrations at given wind speeds are much lower (shown statistically in Table 4) than those measured during Intervals 1 and 3 and are lower than the composite average of Lovett's North Atlantic data set. At the beginning of Interval 2, the radon began to drop to undetectable levels, the barometic pressure changed abruptly, the total water vapor content was near the minimum for the cruise, and the wind direction shifted 180°. All of these observations infer the passage of a frontal system which could have caused the salt peak at 0800 day 39 to be due to advective rather than local processes.

The three prominent wind speed peaks on day 40 are mirrored in the salt aerosol time series but at much lower magnitude than for equivalent wind speeds in Intervals 1 and 3. Coincidentally, our wave height data for this interval (Fig. A-8) also show relatively low amplitudes with respect to observed wind speed. Later in the same interval (0900 - 1500 on day

42), the average wind speed was approximately 12 m/sec but very low values of sea salt aerosol are seen along with relatively lower wave heights. Note that this was an interval of fog, implying stable atmospheric conditions.

Subsequently (0900 day 44 to 0900 day 45), we see a period when the relative humidity dropped from 78% to 53%, the air temperature dropped from 12°C to 6°C, the water vapor content dropped from 10000 to 5000 ppmv, the barometric pressure increased from 748 to 757 torr and the wind attained and held a velocity of 8-10 m/sec. These trends (along with low radon) are indicative of either a subsident cool air mass or an influxing polar air mass, which should have lower advected salt aerosol concentration than the local boundary layer air.

During this entire period the salt load continued to decline, in spite of wind speed increases from below 3 up to 8 or 10 m/sec. This could occur if either no salt was being generated, or the generated salt was not being mixed up to the sampling level. Also note that the wave heights remained at about 1.5 m during the entire period and that all this occurred with the sea water 5°C warmer than the air. Hence, while the air-sea temperature difference indicates unstable atmospheric conditions, the system is responding as though there were no vertical transfer of momentum down to the sea surface, and no upward mixing of generated salt aerosol. The former is inferred from low wave heights, while the latter is inferred from the low and continued decreasing values of observed salt concentrations. The observations that atmospheric stability affects both wave height and vertical fluxes (Austausch coefficient) have been respectively documented by Wiegel (1963), Roll (1965), and Smith (1980).

On day 45, starting at 0900 when the wind speed began rising to 20.6 m/sec., the sea surface quickly responded with higher-amplitude waves, and a salt peak resulted which is considerably broadened compared to other sections of the time series. The persistence of this salt aerosol level in the sampling area may result from either a large number of small-diameter particles in a stationary air mass or advected air with a high salt aerosol concentration. In contrast, the salt aerosol peak centered at 1950 on day 46 occurs during a period of progressively decreasing local wind speed but also coincides with a radon concentration minimum. This latter condition suggests a shift to a more maritime air mass, possibly having a high

residual salt aerosol concentration. If the salt peak on day 45 at 0900 is due to continually sampling the same air mass, the residence time (defined here as in Lovett (1978) to be the time for the salt concentration to drop to "low values" following a wind speed drop) is approximately 19 hours. Lovett's observations of the time variation of sea salt concentration and wind speed indicated "residence times" between 12 and 24 hours. However, for much of our data, the "residence time" of the salt aerosol appears to be about 6 hours. An apparent decrease in the "residence time" might be caused by transiting into an air mass with a lower salt aerosol concentration. Regardless of reason, variations in our salt load decay rate are quite evident.

Rn as a Predictor

If relatively high radon values can be used to indicate shorter travel time over the ocean (i.e. lower fetch and duration), then one would expect a negative correlation between radon concentration and salt aerosol concentration. Examining the trends in both time series yields negative correlations only 60% of the time (39 of 64 comparisons). This would hardly provide a reliable predictive capability for atmospheric salt loadings in this region. Changes in the radon source strength or the north-to-south decrease in land area of the South American continent, when related to the upwind air mass trajectories for this cruise track, could certainly complicate radon-based distinctions between "marine" and"continental" air. Continuously monitoring the salt aerosol particle size distributions would have yielded complimentary information, possibly by indicating the age of the aerosol, to differentiate between local and advected salt components. However this is not a "predictive" scheme, but one to help interpret the current local situation.

Rain, Fog and Ship Spray

During this cruise we encountered periods of fog conditions, precipitation and ship-generated spray. These occurrences are shown along the time axis of the wind speed time series (Figs. 3-5). Scavenging or washout of salt aerosol by precipitation is evident (0900 day 35, 2200 day 39, 0900 day 41 and 0900 day 49), particularly during the rain squalls on day 49. ARCAS data shows an apparent scavenging or washout effect, more

pronounced for drizzle than for fog conditions, due to the particle size capture characteristics of the ARCAS inlet discussed previously. Reductions in salt aerosol concentration from expectedly higher values were also reported by Lovett (1978) in the presence of convection and precipitation.

There were 3 recorded instances of salt spray from the bow which reached the wheelhouse below the ARCAS. Except for the first case on day 35, salt aerosol peaks do not coincide with the reports of spray. Again, the ARCAS discriminates against aerosol particles or droplets larger than fog (including ship-generated spray).

C) Data Interpretation

It can be seen that precipitation removal and advection impose difficulties when trying to match the time series of local wind speed and salt aerosol concentrations. However, in spite of the low correlation coefficients evident in Table 4, we adhered to the approach of Woodcock and Lovett, and examined the sea salt aerosol concentration dependence upon local wind speed using the equation:

$$\ln \theta = a u + b$$

where θ = sea salt aerosol concentration in µg/SCM,

a = slope of linear regression line,

b = intercept of linear regression line,

and u = wind speed in m/sec.

Table 4 lists values for the linear regression equations and Gaussian statistics for the full data set as well as subsets categorized by various sampling or meteorological conditions. The overall statistics for the cruise (Case I in Table 4) indicate that the geometric mean salt aerosol concentration was 11.5 ± 3.0 µg/SCM, and the arithmetic mean wind speed was 9.8 ± 3.9m/sec.

Figure 6 is a scatter diagram of the ARCAS salt data vs. wind speed. It shows the data points used in the analysis and the resulting linear regression equations. Four point sets whose salt values are below 1 $\mu g/m^3$ have been omitted, since they are within 3 σ of the blank for salt

Table 4 — Statistical data on sea salt aerosol and wind speed relationships

Case	Slope a	Intercept b	Correl. Coeff. r	Mean Values $\overline{\ln \theta}$ (μg/SCM)	Mean Values $\overline{u}$ (m/sec)	Std. Dev. $\sigma_{\ln \theta}$	Std. Dev. σ_u	Data Points	Conditions
I	0.093	1.53	0.33	2.44	9.8	1.11	3.9	249	All pairs θ >1μg/SCM
II	0.098	1.53	0.36	2.53	10.1	1.11	4.0	189	Sampling underway
III	0.049	1.71	0.16	2.15	8.9	1.05	3.4	60	Sampling on station
IV	0.096	1.57	0.35	2.54	10.1	1.11	4.0	187	Wind in forward sector
V	0.097	1.82	0.25	2.82	10.3	1.08	2.8	62	Wind in aft sector
VI	0.038	2.50	0.10	2.91	10.7	0.90	2.4	40	Wind in aft sector; underway only
VII	0.100	1.44	0.38	2.43	10.0	1.14	4.3	150	Wind in forward sector; underway only
VIII	0.060	2.57	0.24	3.21	10.7	0.91	3.7	69	Interval #1 (1-69)
IX	0.005	1.87	0.02	1.92	9.4	0.80	3.6	100	Interval #2 (70-171)
X	0.148	1.01	0.53	2.43	9.7	1.21	4.3	80	Interval #3 (172-253)
XI	0.127	1.08	0.28	2.64	12.4	1.18	2.6	153	u> 8m/sec only

Table 4 (Cont'd) — Statistical data on sea salt aerosol and wind speed relationships

Case	Slope a	Intercept b	Correl. Coeff. r	Mean Values		Std. Dev.		Data Points N	Conditions
				$\overline{\ln \theta}$	$\overline{u}$	$\sigma_{\ln \theta}$	σ_u		
XII	0.096	1.44	0.31	2.38	9.8	1.16	3.7	231	Rain removed
XIII	0.108	1.33	0.37	2.33	9.4	1.15	4.0	206	Fog removed
XIV	0.110	1.30	0.36	2.35	9.5	1.17	3.9	189	Rain and fog removed
XV	0.135	0.72	0.53	2.26	11.4	1.24	4.9	44	Rising winds
XVI	0.135	1.11	0.60	2.51	10.4	0.97	4.3	43	Falling winds
XVII	0.097	1.44	0.35	2.40	9.8	1.01	3.7	63	6 hr averaging
XVIII	0.112	1.29	0.37	2.41	9.9	0.86	2.9	15	24 hr averaging

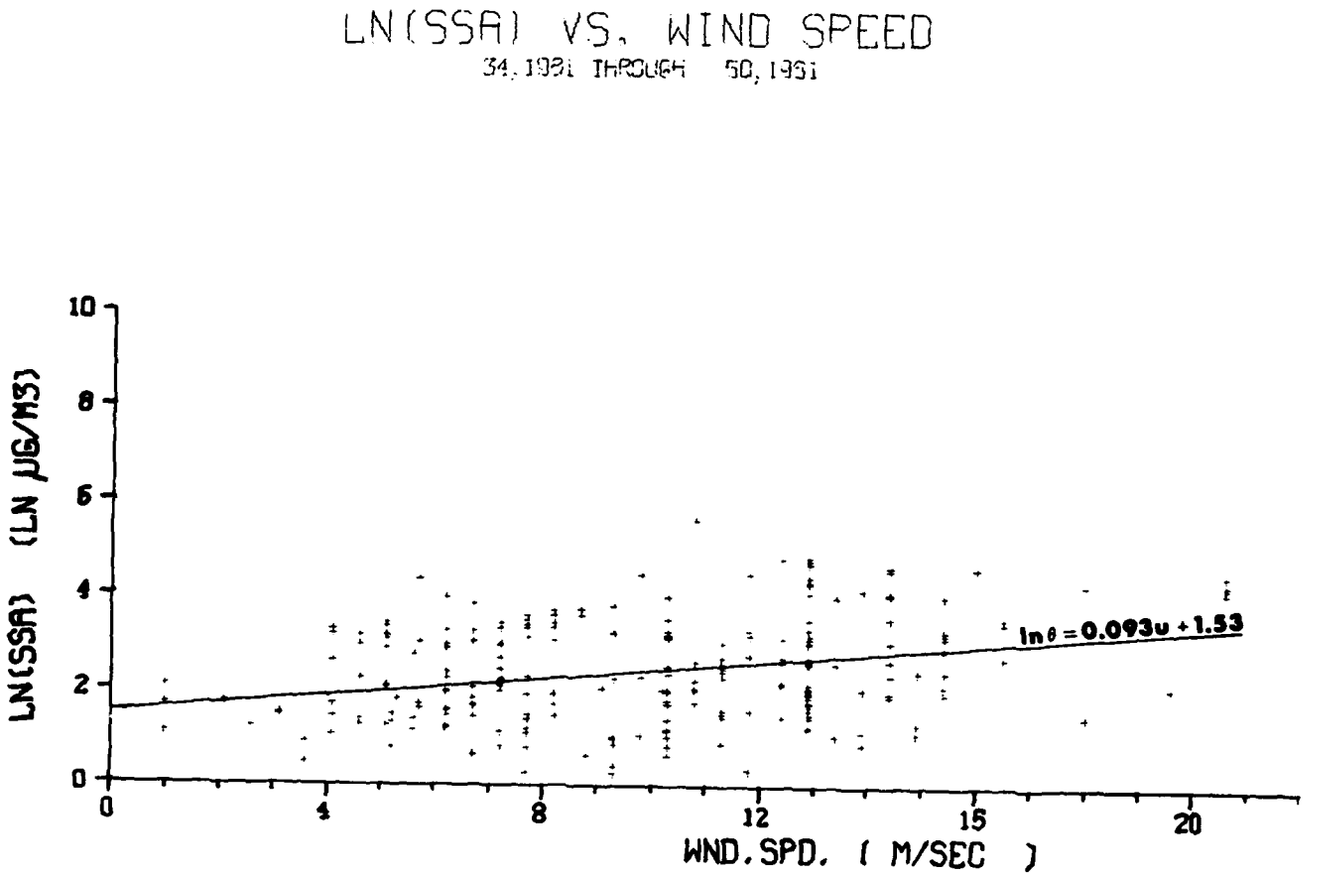

Fig. 6 — Sea salt aerosol concentration vs wind speed data plot with linear regression equation for entire cruise.

determination. The point scatter in Figure 6 is typical for such plots, This has been shown by Lovett, (1975) and Blanchard and Syzdek (1972). In fact, optical measurements of the total volume density of marine aerosol particles (Trusty and Cosden, 1981) show nearly a three-order-of-magnitude range at a given wind speed (5 m/sec). Also, any delay in the response of the sea salt aerosol concentration to increases or decreases in wind speed would further broaden the envelope of values beyond possible scatter caused by drizzle and advection. A delay effect is seen in Table A for samples 176-182 which cover a period of 9 hrs.

Data Reliability

In Cases II through VII, the data has been subdivided to examine possible aerosol sampling bias due to forward ship motion and/or relative wind direction. The first set of comparisons is between aerosol sampling while underway vs. sampling on station (Cases II and III). The most striking differences seen initially are the low slope value (wind dependence) and the very low correlation coefficient for the samples collected while on station. Comparison of these two subsets is difficult since there is a significant difference (>99% by Student's-t test) between the values of the two mean wind speeds. Aerosol data obtained while the relative wind direction was between 270° and 90° (Case IV) and while the relative wind direction was in the opposite quadrants (Case V) show very little difference in their statistics. For data obtained underway, we compared relative wind direction from the aft sector with relative wind from the forward sector (Case VI vs. Case VII). Here one sees some statistically significant differences in salt concentrations and wind speeds. However, these differences should be attributed to real variations in the data subsets rather than those caused by the ship's structure interfering with aerosol transport to the sampler. Such interference would reduce the measured salt aerosol concentration at a given wind speed, but the data does not show this. Also shown in Cases II and III, the wind data does have a bias toward lower speeds while on station than when underway. This is to be expected since stations were not taken in rough weather conditions. Overall, the similarity in the regression analysis parameters for Cases I, II, IV, V and VII, which include the great majority of data points, reaffirms the omnidirectional sampling capability of the ARCAS under the conditions encountered during this cruise.

Interval Statistics

Linear regression parameters for the three intervals discussed previously are presented in Cases VIII - X. Here the relationship between local wind speed and sea salt aerosol concentration varies drastically. Linear regression slopes range from near zero to approximately 0.15 while the respective correlation coefficients vary from near zero to 0.5.

Condensation processes seem to play a decisive roll by incorporating salt aerosol into larger droplets. Under these conditions the upper size limit of particles being sampled will determine the observed salt load. We tried statistical runs with rain and/or fog removed from the data set. These showed no significant improvement in statistics as can be seen in Table 4 (Cases XII-XIV). The statistical manifestation of a condensation/precipitation effect seems to be overshadowed by that of other variables.

Wind Effects and Hysteresis

Advected salt is presumably the hardest component to predict from local observations. Yet advection seems to be the best mechanism to explain the parts of our time series which show salt peaks at times when the wind speed is low or steady. Apparently, either the ship is approaching a zone of generation, or a previously more active air parcel has slowed and the observations are of residual salt in the process of settling out.

Higher correlations were obtained when trying to separate effects of wind generation of aerosol from removal by settling. Salt loads at decreasing wind speeds were separated from the data set as were salt loads at increasing wind speeds. This was done because the mechanisms controlling salt loading should be different at these times. The salt concentrations can increase quite rapidly but seem to decay at about 10 to 16% per hour, measured over periods of 12 to 24 hours. Because of these apparent log-linear changes, we continued to correlate the natural logarithm of salt concentration with wind speed (XV and XVI) in Table 4. Combined subsets of increasing wind speeds (totaling 44 data points) had a correlation coefficient of 0.53, with a slope of 0.14 and intercept of 0.71, while 43 points with decreasing wind speeds gave a correlation

coefficient of 0.61, a slope of 0.10 and an intercept of 1.46. These are markedly better correlated than the overall data. The importance and variability of hysteresis effects is shown by the relatively higher salt loads at lower wind speeds during times of decreasing winds.

In order to test the hypothesis that sampling the salt aerosol for time intervals comparable to previous investigators might improve correlations, we averaged the data over periods of 6 and 24 hours. These statistics are listed in Table 4, Cases XVII and XVIII. There is only a slight improvement in the correlation coefficient for the 6-hour-average data (combining 4 adjacent data points) as compared to the full data set (Case I). Similarly, the 24-hour-average data set shows only a slight improvement over the 6-hour-average data set. It is apparent from the previous results that separating the meteorological processes improves the predictability of the salt aerosol concentration to a better degree than by long-term averaging.

Sea Surface Temperature Effects

In addition to the weather-and sea-state differences among the three intervals of the cruise, there were some distinctive positional sea surface temperature (SST) differences. The respective averages and ranges of the SST's for Intervals 1,2 and 3 were 8°C (2-15°), 3°C (0-12°) and 17°C (12-22°). The lowest correlation coefficient and slope value are associated with the coldest SST's. Blanchard (1963) has demonstrated that the ejection height of jet drops increases with temperature for most of the bubbles in the natural spectrum produced at sea, but temperature effects on the size of film drops are largely unknown. However, we do not believe the temperature effect on bubble production mechanics to be its predominant role of influence.

Mechanisms by which the SST might affect the measured sea salt aerosol concentration are difficult to assess at this point, since large-scale meterological differences are present among the three sampling intervals. However, besides directly affecting bulk water properties such as viscosity and surface tension, the temperature differences between sea water and the overlying air affect the mesoscale meteorology through stability, which in turn influences wave height and vertical mass flux. Thus, SST appears to be an important parameter.

Our data set definitely shows high variability for any simple relationship between local wind speed and sea salt aerosol concentration (over a short time span of 16 days and within an area 17° x 17°) It is possible that this may only reflect unique meteorological conditions during one summer season. Frequency plots of our wind speed data do show some values lower than the prevailing winds for February and some higher than the values for August (winter) in this region of the South Atlantic (Pilot Charts, 1981). The data set was also filtered (Table 4, Case XI) to exclude samples collected at wind speeds less than 8 m/sec. This exercise does result in an increase in the slope when compared to Case I, but the correlation coefficient is unexpectedly lower. Note that this does not represent true winter conditions because the temperature difference between the sea and the air should be different in the winter from that for our February cruise.

Stability Effects

From the foregoing it is apparent that although the wind speed is the driving force for salt generation, other factors complicate a direct link between anemometer readings and salt aerosol concentrations. These factors include condensation effects, advection, and hysteresis effects. Also, the constancy of a salt load equilibrium level at any one measured wind speed seems to be in question due to variations in the stability structure of the atmosphere.

Moreover, the temperature difference between air and sea is apparently not always a sufficient predictor of atmospheric instability. For instance, the following explanation of the time series between day 44 at 0000 to day 45 at 1200 seems to require the theory that atmospheric stability caused the low salt loads observed.

The initial impression was that since the wind shifted to blow against the sea, the waves were reduced, thereby inhibiting the salt generation mechanism. This we believe is an incomplete explanation. First, wind blowing against the direction of wave propagation would have a relative velocity equal to the wind velocity plus the phase velocity of the on coming waves. This should create more stress at the sea surface and increase salt aerosol production. Secondly, the wave directions (not shown) responded to the wind shifts (also not shown) at day 44 at 0900 and

at day 45 at 1200. Thus, the wind was at least partially coupled to the sea surface, but apparently with insufficient time or fetch to make waves greater than 1.5 m. Although we had relatively clean air with little advected salt, the question is, what happened to any salt locally generated by the 10 m/s winds? We believe that no significant amounts were mixed up to sampler height. Due to the coincidence of low waves and low salt concentrations, we believe that low level stability is the cause of this anomalous response to wind speed.

The problem in this case becomes one of attaining stable conditions when the air is 5°C cooler than the sea water. A possible mechanism for this is revealed by Ling et al. (1978), and depends upon the air having low relative humidity with sufficient wind stress to produce sea water droplets and eject them into the air. The mechanism is that evaporating airborne droplets are extracting latent heat (of evaporation) from the atmosphere (instead of the sea). Only the turbulent eddies containing droplets will thereby be cooled and become relatively stable with respect to the surrounding and overlying air. (Our computations show that, under ideal conditions, evaporating 1 gm of water could cool 1 m^3 of air by 2.4°C). Though a temporary phenomenon, this induced stability would selectively inhibit vertical transport of salt mass. Operating below one or two meters, this effect occurs at a height below any usually included in profiles of the marine boundary layer.

Since stability is affected by the SST, it is worth noting that our lowest salt loads occurred during Interval II (when the SST's were lowest), but the average wind speed was almost that of Intervals I and III. We believe that there may be a higher probability for stable atmospheric conditions to exist with lower sea surface temperatures, and this would be in addition to any effects from temperature on bulk water properties. We do not have profiles of atmospheric stability, though they apparently are necessary for both proper data interpretation and salt load prediction.

In spite of this multiplicity of variables, it is instructive to compare our results with those of other investigators whose data has been fit by linear regression. Table 5 lists the resulting slopes and intercepts along with some pertinent measurement information. The slope value for all of our data compares more closely with Toba's calculated slope than with either Woodcock's or Lovett's slopes. If we consider the

Table 5 — Comparison of linear regression parameters for sea salt aerosol studies

Reference	Slope(a)	Intercept(b)	Conditions, Location
Woodcock (1953)	0.16	0.94	600-800m (cloudbase); 20-25°C SST; Hawaii
Lovett (1978)	0.16	1.45	5,10,15m; 10-15°C SST; N. Atlantic, yearly average
Toba (1965)	0.12	---	sea surface, production rate calculated from others
This work (all data)	0.09	1.53	16m; 0-22°C SST; S. Atlantic, summer
This work (Interval 3)	0.15	1.01	16m; 12-22°C SST; S. Atlantic, summer

last 5-day segment of our data (Interval #3) where the SST's are comparable to those of Woodcock and Lovett, the agreement in slope values is much better. Undoubtedly, the relative persistence of the wind systems and the long fetch encountered in the studies by Woodcock and Lovett contribute to the increased concentrations they found. This can be contrasted to greater variability in weather and shorter fetch distances that we experienced in our study.

Noting the relatively good fit of Woodcock's (1953) salt vs wind speed data, one might reflect on the fact that it was necessary for him to estimate wind force (which is done by observing wave and white-cap conditions) from his airplane. Since anemometer measurements were not used, variability in the downward mixing of wind momentum (from anemometer height) does not effect his estimates. It is the overall result of the wind field plus the downward mixing processes that is being evaluated. As previously stated, variations in atmospheric stability seem to affect upward salt transport as well as wave height. It can thereby be inferred that observations which include wave height (as does wind force) might yield better estimates of salt loads than would anemometer-measured wind speeds alone. Since wind force plotted against wind speed gives a somewhat awkwardly shaped curve showing logarithmic tendencies over part of its range, it is also significant that Blanchard and Woodcock (1980) showed the 1953 salt load data to be log-linear with respect to wind speed (in m/sec). This reinforces our observation that the ln of the salt load should be correlated with wind speed, or $\theta = b \cdot e^{a \cdot u}$.

Histograms of Salt Aerosol and Wind Distributions

With a sufficiently long time series, we could presume representative sampling of wind speeds, salt loads, wave heights, and meteorological conditions for an area. The probability distributions and variances of salt loadings, wind speeds, fetches and atmospheric stabilities are expected to be geographical variables.

Early in the analyses, we histogrammed our data to determine the distributions of salt load, wind speed and wave height. From the histograms (Fig. 7) it can be seen that the wind speed distribution is approximately bimodal, with an additional tail on the right. The ln θ is also approximately bimodal, with a larger tail to the right. This extra

FREQUENCY HISTOGRAMS

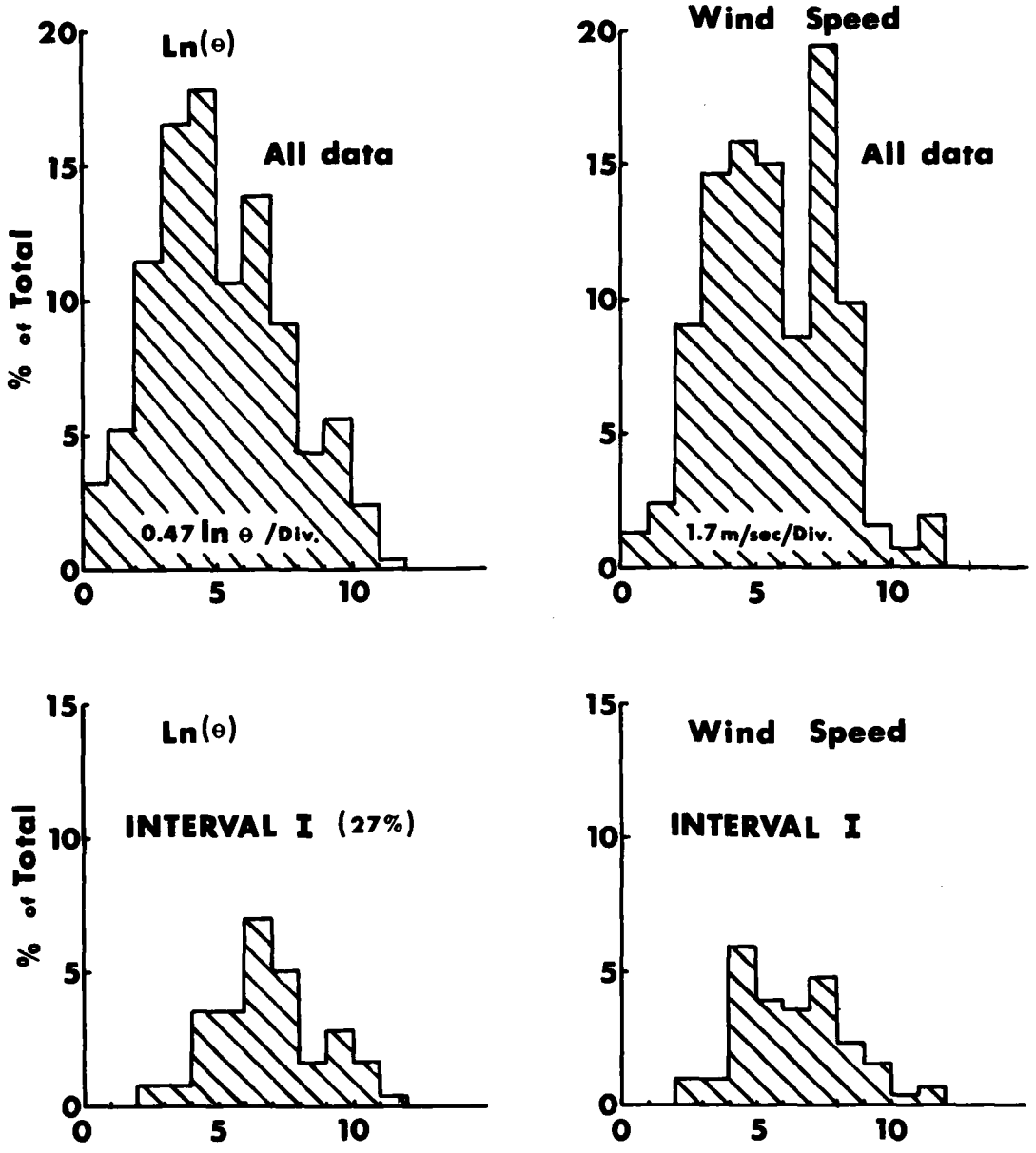

Fig. 7(a) — Frequency histogram of salt aerosol concentration and wind speed for all time series data and each of the three intervals.

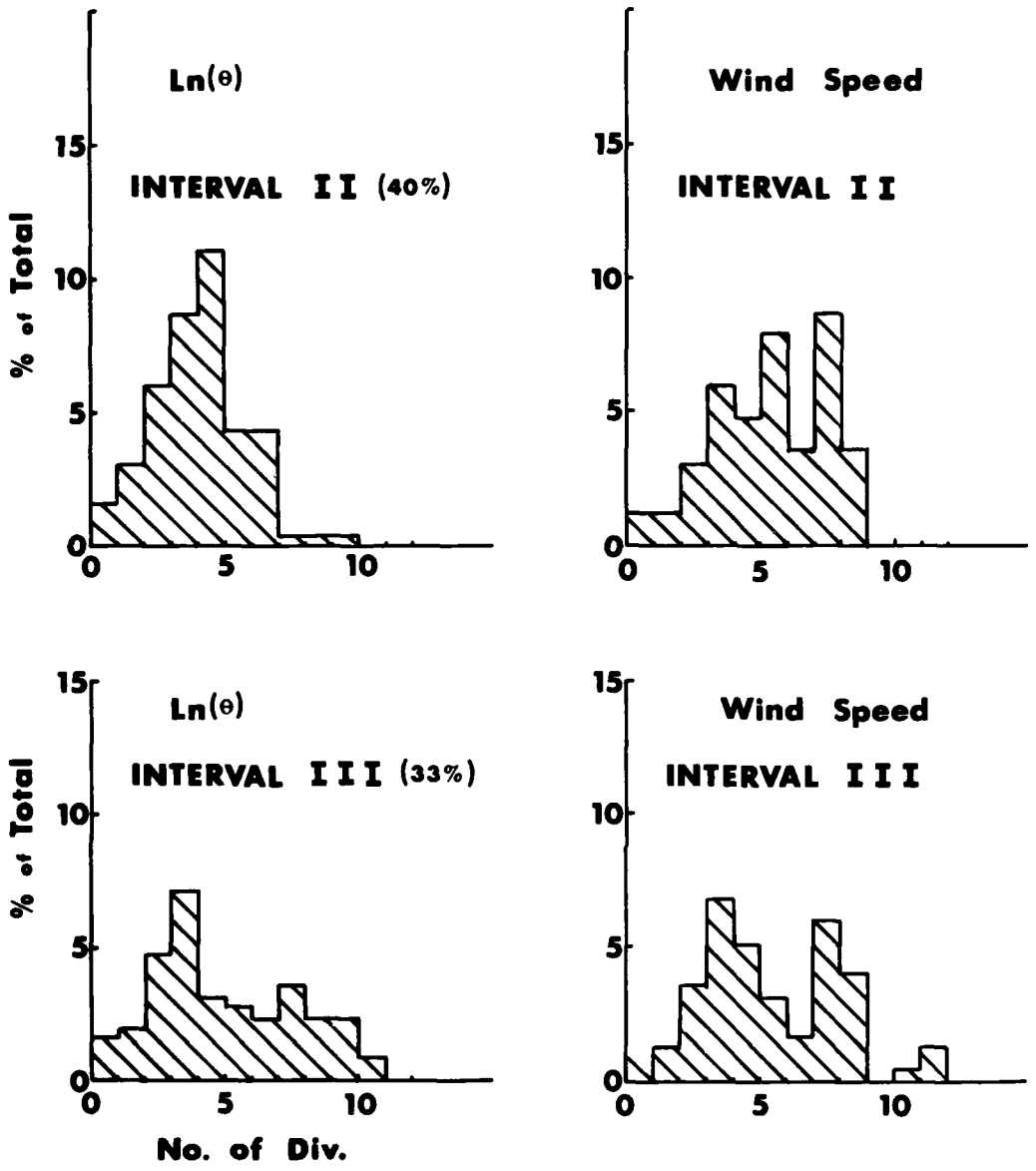

Fig. 7(b) — Frequency histogram of salt aerosol concentration and wind speed.

tailing on ln θ would be difficult to predict from the wind speed distribution. Histograms for Intervals I, II, and III are shown on the same scale as "All data", for comparison.

It can be seen that the salt load distribution mimics the wind speed distribution fairly well, in spite of poor point-by-point correlation of their time series. Comparisons of the histograms can be made by ordering the data and computing the correlations between equally ranked pairs from the ordered data. Table 6 shows the results in Cases XIX-XXIV, where it is apparent that the correlations are greatly improved, once the criterion for sampling coincidence is completely relaxed.

Computer runs on our ordered data yielded correlation coefficients of 0.99 for ln θ vs. wind speed and 0.98 for ln θ vs. wave height. These values may be compared to coefficients of 0.33 and 0.27 for the non-ordered ln θ vs non-ordered wind speed or wave height data, respectively. On the other hand, direct correlation of ordered sea salt aerosol concentration (θ) values with wind speed and wave height yielded lower coefficients (0.84 and 0.90, respectively). These results lead us to the following conclusions. First, the near-perfect correlations of the ordered data indicate that salt load distributions can be estimated from the wind speed or wave height frequency distributions for this area. Secondly, the relationship between salt loading and wind speed (or wave height) is better fit by a log function than by a power function.

So far we have no measurements showing how these functional relationships would vary from one part of the ocean to another. However, the relationships should be sought because general prediction by area (and possibly by season) would alleviate problems of continuous in situ measurements necessary for point-by-point time-wise prediction. Once an area is modelled, the problems due to advection, variations in stability, temperature, and precipitation removal are handled statistically. Thereby, for specific oceanic areas and seasons, a specific cumulative salt loading should be predictable.

A further analytical step can be taken by making linear plots of the cumulative percent distributions of each ordered data set against percentage of time spent sampling. Both axes are thereby normalized. It is immediately apparent from Figure 8 that the ln θ plot corresponds with the wind and wave curves much better than a linear salt concentration (θ)

Table 6 — Sea salt aerosol concentration/wind speed/wave height relationships for ordered data

Case	Slope M	Intercept B	Correl. Coeff. r	Mean Values lnθ	Mean Values u	Std. Dev. $\sigma_{ln\theta}$	Std. Dev. σ_u	#Points N	Conditions
XIX	0.291	-0.42	0.99	2.41	9.8	1.10	3.8	250	lnθ vs. wind speed
XX	0.895	-0.08	0.97	2.39	2.76m	1.15	1.25m	253	lnθ vs. wave height
XXI	0.31	-0.27	0.97	2.76m	9.77	1.25m	3.91	254	Wave height vs. wind speed
XXII	0.24	0.64	0.97	3.21	10.7	0.92	3.7	69	Interval I lnθ vs. wind speed
XXIII	0.22	-0.14	0.96	1.90	9.3	0.80	3.6	102	Interval II lnθ vs. wind speed
XXIV	0.28	-0.36	0.98	2.40	9.7	1.23	4.2	81	Interval III lnθ vs. wind speed

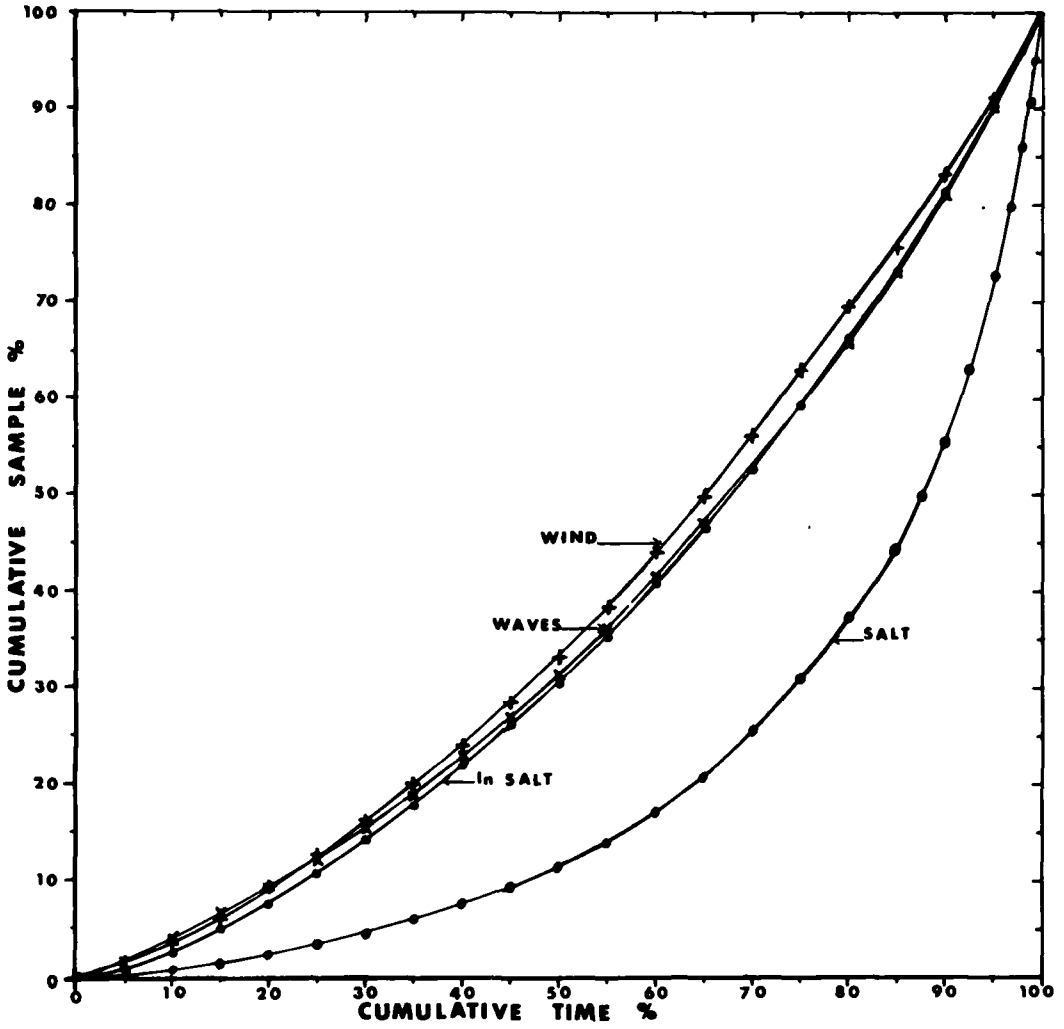

Fig. 8 — Cumulative curves with normalized axes, showing the percentage of total acquired units vs total time spent sampling and/or total number of samples taken.

plot does. The upper plots show a simple curvature which can be nearly removed by taking logs of the variables. This results in

$\log u$ and $\log [\ln \theta]$ or $\theta = e^{(Bu^{M})}$,

where B = 0.16 and M = 1.17 are the intercept and slope of the line fitted to the ordered data above 5 m/sec. With the equation in this form, it does not matter whether one compares $\ln \theta$ to u or some power of u such as u^2 (wind stress) or $u^{3.3}$ (whitecapping; see Monahan, 1971). The exponent (M) of u would include that power. For our case, using

$\theta = e^{Bu^{2M'}}$, M' would equal 0.585. For simplicity, we prefer the former equation with M = 1.17.

It is then required to determine the slopes and intercepts for various areas during various seasons. Although the first thought is to go out and make measurements, we should note that there are relevant data available for many oceanic areas. Wave heights, occurrences of precipitation and fog, and types of cloud cover have been archived, along with wind speeds and directions. The directional data for wind and swell would determine fetch statistics, while any information reflecting stability would be helpful. From the previous discussions one might compare wave height statistics for areas to determine the average degree of wind coupling to the sea surface. Cloud data might be used to estimate vertical circulation and upward mixing. If these prove useful, shorter-term forecasts might be made using satellite data. Furthermore, it should become clear from the analysis which oceanic areas represent extremes where measurements should be made for improved modelling.

Wind Velocity Profiles and Data Scatter

Under neutral conditions, wind velocity profiles are usually presumed to be "log" or "log + linear" in form. However, neutral conditions are not universal and only field measurements will show the true profile. Various authors show the aerodynamic drag coefficient (C_d) to vary by factors up to 3 for any one wind speed, and by a factor of 6 for the range of wind speeds of interest here (Smith, 1980; Brocks and Krugermeyer, 1972). Although the C_d is a function of atmospheric variables, it can be taken as an efficiency factor for mixing horizontal momentum down to the sea surface.

Smith (1980) found that for long-fetch waves, doubling the drag coefficient quadrupled the wave height, approximately in a linear fashion.

It is now not suprising that the scatter in drag coefficient vs. wind speed found in Smith's paper is of nearly the same distribution and magnitude as the scatter in our ln θ vs. wind speed. (Recall that while the resulting surface stress is linearly related to the coefficient of drag, it is proportional to the square of the wind speed.)

Rationale for Ln θ vs. u

We believe that ln θ is best matched to u because θ is the product of a number of random variables with wind speed as the main driving force. We also believe that this relationship holds for short-term as well as long-term sampling because it appears that, regardless of white cap coverage, upward mixing would still be a variable which is controlled by the structure of the turbulent boundary layer (more specifically, by the integral scale of the turbulent eddies). We submit that it is the randomness from mixing by turbulent eddies that makes the sampled salt load the result of a string of conditional probabilities. These conditional probabilities have values and ranges set by meteorological conditions, and their combining rules transform linear distributions into logarithmic ones (or normal distributions into log-normal ones).

A constant set of conditional probabilities for each step in the black box model should give a somewhat logarithmic distribution to any set of aerosol samples when all are taken at the same wind speed. A distribution of wind speeds should give us an ensemble of samples whose distribution would be either logarithmic or like that of the wind speed, depending on which has the greater variance. In any case, it is expected that at least the ends of the salt aerosol distribution would be logarithmic.

If one now varies the meteorological conditions so that the conditional probabilities for each step vary over the duration of the experiment, the scale of these variations might far exceed that of the wind speed in affecting the sampled aerosol salt distribution. It is believed that this is the effect that produced the extreme logarithmic skewness in our salt aerosol data.

CONCLUSIONS

A simple physical relationship does not exist between synoptic measurements of wind speed and sea salt aerosol concentrations in the marine atmosphere. This is due to the effects of hysteresis, condensation processes and the varying structure of the turbulent boundary layer. In this region of the South Atlantic Ocean, the low correlation between sea salt aerosol concentration and local wind speed is attributed to the high variability of the above-mentioned effects. Removing the temporal constraint by ordering both data sets results in an extremely high (r = 0.99) correlation coefficient. This gives promise for the estimation of salt aerosol distributions from wind speed distributions for specific oceanic areas and seasons. For our study area, the equation $\theta = e^{Bu_M}$ seems to best encompass the statistical and deterministic parameters for the aerosol concentration distributions.

There seem to be systematic differences in sea salt aerosol concentrations related to locations having significantly different sea surface temperatures. We believe that the predominant effect of sea surface temperature pertains to the formation of stable or unstable conditions in the marine boundary layer.

Wave features may be useful for enhancing the accuracy of real-time estimates of the salt aerosol concentration since the composite wave spectrum contains a history of the previous wind and reflects the degree of coupling with the local winds.

Measurements using two samplers which had different upper range particle size cutoffs indicated that during rain and fog, a large percentage of airborne salt near sea level shifts from aerosol-sized particles to droplets greater than approximately 50 μm diameter (upper range of fog droplets). Consequently, the determination of the total concentration of atmospheric salt would require special sampling techniques to deal with both wet and dry particles of all sizes.

Atmospheric radon determinations, made concurrently with the automated aerosol samplings, corroborated and enhanced the information provided by satellite streamfunction analysis. The radon data was particularly useful in identifying non-continental, subsident or advected air masses which also had very low salt aerosol concentrations. These conditions accounted for 15% of the total sampling time and explained two episodes where the local

wind was moderately strong (10-15 m/sec) but the actual salt aerosol concentration was unexpectedly low.

RECOMMENDATIONS

More research in diverse regions is necessary to obtain quantitative information on the variability in sea salt aerosol concentration and related parameters before reliable predictive models can be formulated. For the near future, the prediction of salt aerosol concentration should be modelled on a statistical basis using available data. This exercise may lead to reliable generalizations for easily categorized oceanic regimes.

A real-time prediction capability for salt aerosol concentration is expected to take longer to develop. Eventually, such a capability could be based on regional models whose parameters are modified by synoptic satellite observations.

Any future field studies should include similar meteorological measurements at two or three elevations to determine vertical fluxes, atmospheric stability and mixing parameters near the sea surface. Other factors, such as water temperature, directional wave height spectra, and whitecap coverage, should be monitored nearly continuously and automatically throughout the experiment. Unfortunately, reliable measurements of some of these parameters are extremely difficult to make from a moving ship. For shipboard sampling, the height of the sampler inlet relative to the wave tops should also be monitored. Additionally, much beneficial ancillary information could be provided by continuous measurement of particle sizes at two elevations.

ACKNOWLEDGMENTS

The streamfunction charts were obtained through the courtesy of Joseph Mullaney and John Strong of the Forecast Division, National Weather Service of the National Oceanic and Atmospheric Administration. We are also indebted to Andre Robinson, Katherine Schwarz and Joseph Liu for laboratory assistance in processing and analyzing the aerosol samples and in meteorological data reduction. The manuscript has also benefitted from comments by Kingsley Williams, Duncan Blanchard and Joseph Prospero. The authors wish to thank Clifford Gordon, Clifford Trump, Gaspar Valenzuela, Richard Mied, William Plant, Benn Okawa and John Dugan for instructive discussions and for the loan of valuable reference materials. Final typing of the manuscript was performed by Peg Szymczak, whose diligence is greatly appreciated.

REFERENCES

Atlas of Pilot Charts (1981). South Atlantic Ocean. Defense Mapping Agency Pub. 105, Washington, DC 20315.

Barger, W. R. and W. D. Garrett (1970). Surface Active Organic Material in the Marine Atmosphere. J. Geophys. Res. 75, 4501-4566.

Blanchard, D. C. (1963). The Electrification of the Atmosphere by Particles from Bubbles in the Sea. Progress in Oceanography 1, Academic Press, N.Y., pp 71-202.

Blanchard, D. C. and L. Syzdek (1972). Variations in Aitken and Giant Nuclei in Marine Air. J. Phys. Oceanogr. 2, 255-262.

Blanchard, D. C. and A. H. Woodcock (1980). The Production, Concentration, and Vertical Distribution of the Sea-Salt Aerosol. Ann N.Y. Acad. Sci. 338, 330-347.

Bressan, D. J. (1981). Maritime Atmosphere Salt Load Monitoring System. Naval Research Laboratory Memorandum Report 4581, 41 pp.

Brocks, K. and L. Krugermeyer (1972). The Hydrodynamic Roughness of the Sea Surface. Chapter 5 in Studies in Physical Oceanography, Vol. 1, p 75-92. A. L. Gordon, (Ed.), Gordon and Breach, N.Y.

Garrett, W. D. (1968). The Influence of Monomolecular Surface Films on the Production of Condensation Nuclei from Bubbled Sea Water. J. Geophys. Res. 73, 5145-5150.

Graham, W. F., S. R. Piotrowicz and R. A. Duce (1979). The Sea as a Source of Atmospheric Phosphorous. Marine Chem. 7, 325-342.

Guedalia, D., A. Lopez, J. Fontan and A. Birot (1972). Aircraft Measurements of Rn-222, Aitken Nuclei and Small Ions up to 6 km. J. Appl. Meteor. 11, 357-365.

Hochrainer, D. (1978). Physical Behavior and Sampling of Airborne Particles. Chapter in Analysis of Airborne Particles by Physical Methods. H. Melissa, ed. CRC Press pp 7-26.

Hoover, J. B. (1982). The METEOR Software Package for Analysis of Meteorological Data. Naval Research Laboratory Memorandum Report 4674, 83 pp.

Larson, R. E. (1973). Measurement of Radioactive Aerosols using Thin Plastic Scintillators. Nuclear Inst. Methods 108, 467-470.

Larson, R. E. and D. J. Bressan (1978). Automatic Radon Counter for Continual Unattended Operation. Rev. Sci. Inst. 47, 965-969.

Larson, R. E. and D. J. Bressan (1980). Air Mass Characteristics over

Coastal Areas as Determined by Radon Measurements. Preprint Volume: Second Conf. Coastal Meteorology. Jan 30-Feb 1, 1980. AMS, Boston, Mass. p. 84-100.

Lepple, F. K. (1975). Eolian Dust over the North Atlantic Ocean. Ph.D. Dissertation Unvi. of Delaware, Newark, 270 pp. (Univ. Microfilm, Ann Arbor, Mich. #75-14,966).

Lepple, F. K., R. E. Ruskin and W. A. Von Wald (1980). Sea Salt Aerosol Measurements Aboard GTS CALLAGHAN. Naval Research Laboratory Memorandum Report 4373, 68 pp.

Ling, S. C., A. Saad, and T. W. Kao (1978). Mechanics of Multiphase Fluxes over the Ocean. Paper in Turbulent Fluxes through the Sea Surface, Wave Dynamics, and Prediction, p. 185-197. A. Favre and K. Hasselmann (eds.), Plenum Press, N.Y.

Lockhart, L. B. Jr. (1960). Atmospheric Radioactivity in South America and Antarctica J. Geophys. Res. 65, 3999-4005.

Lovett, R. F. (1975). The Occurrence of Airborne Sea-Salt and its Meteorological Dependence. M. Sci. Thesis, Heriot-Watt University, U.K., 195 pp.

Lovett, R. F. (1978). Quantitative Measurement of Airborne Sea-Salt in the North Atlantic. Tellus 30, 358-364.

McRae, G. J. (1980). A Simple Procedure for Calculating Atmospheric Water Vapor Concentration. Air Poll. Contr. Assoc. J. 30, 394.

Monahan, E. C. (1971). Oceanic Whitecaps. J. Phys. Oceanogr. 1, 139-144.

Parkin, D. W., D. R. Phillips and R. A. L. Sullivan (1970). Airborne Dust Collections Over the North Atlantic. J. Geophys. Res. 75, 1782-1793.

Paterson, M. P. and K. T. Spillane (1969). Surface Films and the Production of Sea-Salt Aerosol. Quart J. Royal Meteor. Soc. 95, 526-534.

Piotrowicz, S. R., R. A. Duce, J. L. Fasching and C. P. Weisel (1979). Bursting Bubbles and Their Effect on the Sea-to-Air Transport of Fe, Cu and Zn. Marine Chem. 7, 307-324.

Prospero, J. M. (1979). Mineral and Sea Salt Aerosol Concentrations in Various Ocean Regions. J. Geophys. Res. 84, 725-731.

Riley, J. P. and R. Chester (1971) Introduction to Marine Chemistry, Academic Press, N.Y., 465 pp.

Roll, H. U. (1965). Physics of the Marine Atmosphere, Academic Press, N.Y.

Savoie, D. L. and J. M. Prospero (1977). Aerosol Concentration Statistics for the Northern Tropical Atlantic. J. Geophys. Res. 82, 5954-5964.

Smith, S. D. (1980). Wind Stress and Heat Flux over the Ocean in Gale Force Winds. J. Phys. Oceanogr. 10, 709-726.

Toba, Y. (1965). On the Giant Sea-Salt Particles in the Atmosphere. I. General Features of the Distributions. Tellus 17, 131-145.

Trusty, G. L. and T. H. Cosden (1981). Optical Extinction Predictions from Measurements aboard a British Weather Ship. Naval Research Laboratory Report 8497, 46 pp.

Tsunogai, S., O. Saito, K. Yamada and S. Nakaya (1972). Chemical Composition of Oceanic Aerosol. J. Geophys. Res. 77, 5283-5292.

Wiegel, R. L. (1963). Some Engineering Aspects of Wave Spectra. Chapter 5 in Ocean Wave Spectra p 309-321. Conference Proceedings, Easton, MD. Prentice Hall Publishers, Englewood Cliffs, NJ.

Wilkening, M. H. and W. E. Clements (1975). Radon 222 from the Ocean Surface. J. Geophys. Res. 80, 3828-3830.

Wilkniss, P. E., R. E. Larson, D. J. Bressan and J. Steranka (1974). Atmospheric Radon and Continential Dust near the Antarctic and their Correlation with Air Mass Trajectories Computed from Nimbus 5 Satellite Photographs. J Appl. Meteor. 13, 512-515.

Woodcock, A. H. (1953). Salt Nuclei in Marine Air as a Function of Altitude and Wind Force. J. Meteorol. 10, 362-371.

Wu, J. (1981). Evidence of Sea Spray Produced by Bursting Bubbles, Science 212, 324-326.

Appendix

General Circulation Patterns in Study Area

Day 32 (Feb. 1, 1981): From the streamfunction analyses, the ship is between a circumpolar flow bringing clean maritime air rapidly across South America and a counterclockwise flow of maritime air around an anticyclone in the South Atlantic. Shipboard wind measurements show the wind direction changing from west to east late in the day, followed by a return to a westerly direction on the following day. The decrease of radon to near zero on day 32 followed by an increase on day 33 is consistent with this pattern.

Day 33: The westerly flow of air in the morning is replaced by a poorly defined flow of air moving from west to southwest, parallel to the coast of South America.

Days 34 and 35: The air flow veers to westerly on the 34th and then back to southerwesterly throughout day 35.

Day 36: The streamfunction analysis shows air flowing over southern South America from the southwest and then southeastward over the ship location. This is generally in agreement with the shipboard wind measurements and the low radon concentrations encountered.

Day 37: By 1200 GMT, the air reaching the ship had more of a continental history as a result of counterclockwise circulation around an anticyclone. This high-pressure system had moved from over the land in a southeasterly direction and was centered around 35°S and 50°W at 1200 GMT.

Day 38: The air flow from the continent continues. By 1800 GMT, the anticyclone is centered around 40°S and 36°W. The southward course of the ship places it in air with progressively less time spent over land during transit over South America.

Days 39 and 40: The ship has moved out of the area covered by

streamfunction analysis but indications from the charts in the region just north of the ship indicate that there would be little if any continental history of the air. Radon concentrations
decreasing from 0.5 pCi/m^3 to near zero values substantiate this trend.

Day 41: The increase in radon is consistent with a westerly flow of air from the South American continent.

Day 42: The shipboard wind data suggests that the radon peak (2.2 pCi/m^3) may have been associated with a frontal system which is not indicated on the streamfunction analysis charts.

Day 43 and 44: Streamfunction analysis indicates a general westerly or southwesterly flow which should have picked up some continental air but the shipboard winds on day 44 show a wind change from northwesterly to southwesterly late in the day.

Day 45: The analysis predicts mostly maritime air with some increasing land crossings in late afternoon. This trend is followed in the radon data.

Day 46: The flow of air from the westnorthwest at 0000 GMT brings in a substantial continental component to the region of the ship. By 1200 GMT, the flow is from the southwest, implying a smaller continental component.

Day 47: The ship is moving northward and the westerly air flow results in higher radon concentrations as this wind trajectory covers more land area. By afternoon, the ship may be encountering a frontal system and/or a counterclockwise flow of maritime air around a weak anticyclone near 30°S and 30° to 40°W. This is evidenced by very low radon values after 1200 GMT.

Days 48 and 49: Streamfunction analysis is not will defined at this time in the area of the ship. On these days, the radon concentration is about the only indicator of air mass history and it shows two more

injections of continentally derived air.

Day 50: After some mixing with maritime air, the continental component steadily increases as the ship approaches land and the radon concentration reaches its maximum concentration of 12.5 pCi/m^3 at Mar del Plata, Argentina.

Table A — Sea salt aerosol concentration and selected environmental data

Sample No.	JD	GMT	Salt Conc. (μg/SCM)	Wind Speed (m/sec)	Temp. (°C) Air	Temp. (°C) Sea#
1	034	1504	4.3	8.2	18.7	16
2		1634	24.3	11.8	15.8	15
3		1804	23.5	10.3	17.7	15
4		1934	3.3	7.7	14.0	14
5		2104	7.5	12.9	14.1	13
6		2234	8.4	15.4	15.0	13
7	035	0004	72.5	18.0	14.0	13
8		0134	93.2	20.6	13.4	13
9		0304	64.8	20.6	12.7	13
10		0434	35.5	14.4	11.0	13
11		0604	98.1	14.4	11.9	13
12		0734	101.2	16.0	11.9	12
13		0904	31.8	16.5	12.0	13
14		1033	35.6	16.5	12.5	13
15		1203	15.5	16.5	12.5	13
16		1334	25.4	15.4	13.5	13
17		1503	22.8	12.9	12.7	13
18		1633	20.8	12.9	12.3	13
19		1802	21.1	11.3	11.3	13
20		1932	25.7	9.3	13.4	12
21		2102	28.8	5.1	13.3	12
22		2232	28.8	4.6	11.3	12
23	036	0002	24.4	4.1	11.2	12
24		0132	19.7	4.6	11.1	12

Table A (Cont'd) — Sea salt aerosol concentration and selected environmental data

Sample No.	JD	GMT	Salt Conc. (μg/SCM)	Wind Speed (m/sec)	Temp. (°C) Air	Sea#
25	036	0302	30.6	5.1	10.7	13
26		0431	30.9	7.2	11.0	11
27		0601	32.7	7.7	11.1	12
28		0731	36.4	7.7	10.4	14
29		0901	45.5	6.7	10.9	12
30		1031	27.8	7.2	10.3	9
31		1201	23.3	7.7	11.0	9
32		1331	36.2	8.2	12.0	11
33		1501	30.6	8.2	11.0	10
34		1630	86.4	9.8	10.7	9
35		1801	54.3	10.3	10.5	8
36		2000	279.8	10.8	10.4	7
37		2124	90.8	11.8	11.0	7
38		2254	23.3	12.4	10.5	7
39	037	0024	9.1	12.4	10.5	7
40		0154	15.2	12.4	10.1*	7
41		0324	16.0	11.8	9.8*	7
42		0454	13.7	10.8	9.5*	7
43		0624	9.6	9.3	9.1*	7
44		0754	9.9	7.7	8.8*	7
45		0924	20.2	7.2	8.5*	7
46		1054	15.1	7.2	8.2*	6
47		1224	8.0	6.7	7.9	6
48		1354	11.2	6.2	8.0	5
49		1524	21.1	6.7	8.0	5
50		1654	29.6	7.7	9.2	5
51		1824	27.6	7.7	9.1	5
52		1954	21.2	8.2	9.2	5
53		2124	2.7	9.3	9.6	5
54		2254	7.6	10.3	10.0	5

Table A (Cont'd) — Sea salt aerosol concentration and selected environmental data

Sample No.	JD	GMT	Salt Conc. (μg/SCM)	Wind Speed (m/sec)	Temp. (°C) Air	Sea#
55	038	0024	6.8	14.4	9.0	5
56		0154	7.2	15.4	8.6	5
57		0325	13.8	12.4	7.8	5
58		0455	24.6	10.3	7.3	5
59		0625	23.1	10.3	7.6*	5
60		0755	9.4	10.8	7.1*	5
61		0926	11.4	11.3	6.6*	5
62		1056	13.5	11.3	6.2*	5
63		1226	126.2	12.4	6.0	4
64		1356	111.8	12.9	5.6	3
65		1526	123.5	12.9	5.4	4
66		1656	120.4	12.9	5.2	3
67		1826	73.2	12.9	5.6	3
68		1956	45.0	8.3	5.7	3
69		2126	26.6	6.2	6.1	3
70		2256	3.4	6.2	5.6	3
71	039	0026	9.7	6.2	6.6	3
72		0156	5.2	5.7	3.8	3
73		0326	23.7	5.1	3.9	3
74		0456	19.7	6.2	3.6*	3
75		0626	20.9	5.7	3.4*	3
76		0756	22.0	5.1	3.3*	3
77		0926	23.6	5.1	3.2*	3
78		1056	52.7	6.2	3.1	3
79		1226	79.4	5.7	3.1	2
80		1356	8.3	5.1	3.1	1
81		1526	7.9	5.1	3.0	2
82		1656	7.3	6.2	3.5	2
83		1826	8.8	7.2	3.0	2
84		1956	9.4	7.2	2.6	2
85		2126	6.8	7.7	3.4	1
86		2256	4.3	11.3	3.5	1
87	040	0026	10.6	14.4	1.9	1

Table A (Cont'd) — Sea salt aerosol concentration and selected environmental data

Sample No.	JD	GMT	Salt Conc. (μg/SCM)	Wind Speed (m/sec)	Temp. (°C) Air	Sea#
88	040	0156	11.3	15.4	2.1	1
89		0326	7.9	13.9	2.0	1
90		0456	7.5	10.3	1.7	0
91		0626	10.7	10.3	1.8	0
92		0756	12.3	11.3	1.5	0
93		0927	8.8	12.4	1.1	0
94		1058	8.6	12.4	1.9	0
95		1228	7.6	10.2	1.9	0
96		1358	8.0	9.1	2.2	0
97		1528	10.1	9.8	2.5	0
98		1658	7.5	10.3	2.4	0
99		1828	5.7	10.3	2.5	0
100		1958	6.9	8.2	2.6	0
101		2125	5.6	5.7	3.0*	0
102		2258	4.4	3.1	2.1	1
103	041	0028	3.6	5.1	2.2	1
104		0158	5.3	6.7	1.9	1
105		0456	4.1	10.3	1.9	1
106		0626	4.3	12.4	2.1	0
107		0756	8.0	12.9	2.7	0
108		0926	3.6	12.9	3.2	0
109		1056	4.7	12.9	3.5	0
110		1226	6.0	12.9	2.9	0
111		1356	7.2	12.9	3.1	1
112		1526	2.9	13.4	3.6	1
113		1656	2.5	13.9	4.2*	1
114		1826	3.1	14.9	4.8*	1
115		1956	3.8	14.9	5.4*	2
116		2126	5.9	12.9	6.1	2
117		2256	13.6	12.9	6.0	2
118	042	0026	7.3	14.4	6.2	2

Table A (Cont'd) — Sea salt aerosol concentration and selected environmental data

Sample No.	JD	GMT	Salt Conc. (μg/SCM)	Wind Speed (m/sec)	Temp (°C) Air	Temp (°C) Sea#
119	042	0156	18.4	15.4	4.0	2
121		0456	13.7	12.9	4.6	2
123		0756	7.6	10.8	5.4	2
124		0926	10.1	11.3	5.6	2
125		1056	2.5	11.3	5.8	2
126		1226	4.7	11.3	5.9	2
127		1356	1.4	11.8	7.1	2
128		1526	5.1	11.8	5.9	2
129		1656	8.8	12.9	5.7	2
130		1826	6.6	12.9	6.3	2
131		1956	7.1	12.9	6.5	2
132		2126	8.1	12.9	5.8	2
133		2256	24.9	12.9	6.0	2
134	043	0026	28.2	12.9	6.5	3
135		0156	13.7	12.9	6.7*	3
136		0326	15.3	12.9	6.9	3
137		0456	21.3	12.9	7.1*	3
138		0626	15.2	11.3	7.3*	4
139		0756	12.8	10.3	7.6*	5
140		0926	25.2	9.3	7.9*	4
141		1056	9.5	7.2	8.2*	3
142		1126	8.2	7.2	8.5*	3
143		1356	6.3	6.7	7.9	4
144		1526	4.8	6.2	8.3	4
145		1656	7.1	6.2	9.8	6
146		1826	17.9	6.2	8.4	7
147		1956	18.4	5.1	9.6*	8
148		2126	4.3	3.1	10.8	9
149		2256	5.5	1.0	12.0	10
150	044	0025	8.2	1.0	11.6	7

Table A (Cont'd) — Sea salt aerosol concentration and selected environmental data

Sample No.	JD	GMT	Salt Conc. (μg/SCM)	Wind Speed (m/sec)	Temp. (°C) Air	Sea#
151	044	0155	3.4	2.6	11.1	7
152		0325	2.5	3.6	10.8	7
153		0455	3.0	1.0	9.1	8
154		0625	5.6	4.1	9.8	9
155		0755	4.2	6.7	10.2*	10
156		0925	4.1	7.7	10.6*	11
157		1055	3.1	7.2	11.0	11
158		1225	2.8	9.3	10.7	12
159		1355	1.9	8.8	7.6	11
160		1525	2.2	7.7	8.2	11
161		1655	2.4	9.3	9.7	11
162		1825	2.9	9.8	7.9	11
163		1955	2.8	10.3	7.8	11
164		2125	3.2	10.3	6.3	12
165		2255	3.3	10.3	6.3*	12
166	045	0025	2.3	10.3	6.4	12
167		0155	1.9	10.3	6.6	12
168		0325	1.5	9.3	6.8	12
169		0455	1.3	7.7	8.1	12
170		0625	0.9	7.7	10.7	12
171		0755	0.6	6.7	9.6	12
172		0925	1.9	6.7	10.7	12
173		1055	0.4	7.7	11.1	12
174		1225	1.3	9.3	13.7	12
175		1355	4.9	11.8	15.8	12
176		1525	3.2	13.9	15.8*	13
177		1655	4.5	18.0	15.9*	13
178		1825	8.5	19.6	16.0*	13
179		1955	71.6	20.6	16.1*	13
180		2125	77.3	20.6	16.2*	13
181		2255	56.5	15.4	16.3	14

Table A (Cont'd) — Sea salt aerosol concentration and selected environmental data

Sample No.	JD	GMT	Salt Conc. µg/SCM)	Wind Speed (m/sec)	Temp. (°C) Air	Sea#
182	046	0024	64.3	13.9	16.5	14
183		0153	85.2	12.9	16.9	14
184		0323	129.4	12.9	17.0*	14
185		0452	59.9	12.9	17.0*	14
186		0522	76.4	12.9	17.0*	14
187		0751	55.5	13.4	17.0*	14
188		0920	60.5	14.4	17.0*	14
189		1020	27.3	15.4	17.0*	14
190		1219	23.5	15.4	17.0	15
191		1349	11.4	14.9	17.6	16
192		1518	4.4	12.9	18.0	17
193		1648	3.4	12.9	18.1	16
194		1817	14.3	12.9	16.4	15
195		1947	26.9	11.8	17.0	15
196		2116	19.7	7.2	17.1	16
197		2246	6.3	5.3	16.6	17
198	047	0015	4.9	4.1	15.8	17
199		0145	13.8	4.1	16.0	17
200		0315	27.4	4.1	15.8	17
201		0445	15.9	5.6	16.1	18
202		0615	20.5	6.7	16.1	18
203		0745	33.7	10.3	15.4	19
204		0915	105.7	14.4	15.2	19
205		1046	59.3	14.4	16.0	18
206		1216	14.3	14.4	15.6	18
207		1345	13.4	13.4	17.0	18
208		1514	7.9	10.8	16.5	18
209		1644	5.8	10.8	17.4	18
210		1814	6.0	10.3	17.0	18
211		1944	5.5	8.2	16.8	18
212		2113	4.5	5.2	16.4	18
213		2243	3.6	4.6	16.6	18
214	048	0012	4.0	4.6	16.7*	18
215		0141	3.2	5.6	16.9*	18
216		0311	3.0	7.7	17.1*	18

Table A (Cont'd) — Sea salt aerosol concentration and selected environmental data

Sample No.	JD	GMT	Salt Conc. (μg/SCM)	Wind Speed (m/sec)	Temp. (°C) Air	Sea#
217	048	0441	4.5	7.7	17.3*	18
218		0610	4.0	7.7	17.5*	18
219		0740	25.8	6.7	17.7*	18
220		0910	0.0	3.1	17.9*	18
221		1039	4.5	3.1	18.0*	18
222		1209	2.9	4.1	22.7	21
223		1338	2.2	5.2	22.5*	22
224		1508	3.8	5.2	21.0*	22
225		1638	3.3	6.2	21.5	22
226		1808	4.4	6.2	21.4	22
227		1938	18.4	6.2	21.2	22
228		2108	3.4	6.2	21.0	22
229		2238	9.8	4.6	22.0	22
230	049	0008	11.8	7.2	23.2	22
231		0138	24.1	10.3	22.7	22
232		0308	26.1	10.3	22.2	22
233		0438	40.2	8.2	22.4	22
234		0608	5.6	10.3	23.3	22
235		0738	7.5	12.9	21.9	23
236		0908	5.4	12.9	20.0	22
237		1038	7.9	12.9	20.6	22
238		1208	112.9	12.9	20.8	22
239		1338	77.3	12.9	20.5	22
240		1508	33.9	12.9	19.5	22
241		1638	27.6	8.2	15.7	17
242		1808	36.8	8.7	16.9	14
243		1938	41.4	8.7	20.6	14
244		2108	8.4	7.2	18.4	14
245		2238	5.4	6.7	16.0	14
246	050	0008	4.9	6.2	15.0*	16
247		0138	4.0	5.6	16.2	16
248		0308	4.3	4.1	16.1	17
249		0438	5.8	2.1	16.3	17
250		0608	1.6	3.6	16.4	17
251		0738	2.3	7.2	17.0	17
252		0908	1.9	6.7	13.7	17

Table A (Cont'd) — Sea salt aerosol concentration and selected environmental data

Sample No.	JD	GMT	Salt Conc. (μg/SCM)	Wind Speed (m/sec)	Temp. (°C) Air	Temp. (°C) Sea#
253	050	1038	7.3	7.2	14.5	17

*Denotes interpolated air temperatures to compensate for gaps in data logger output caused by power outages or electrical interference.
#Surface water temperature obtained from ship's sea chest and entered in log every 2 hours.

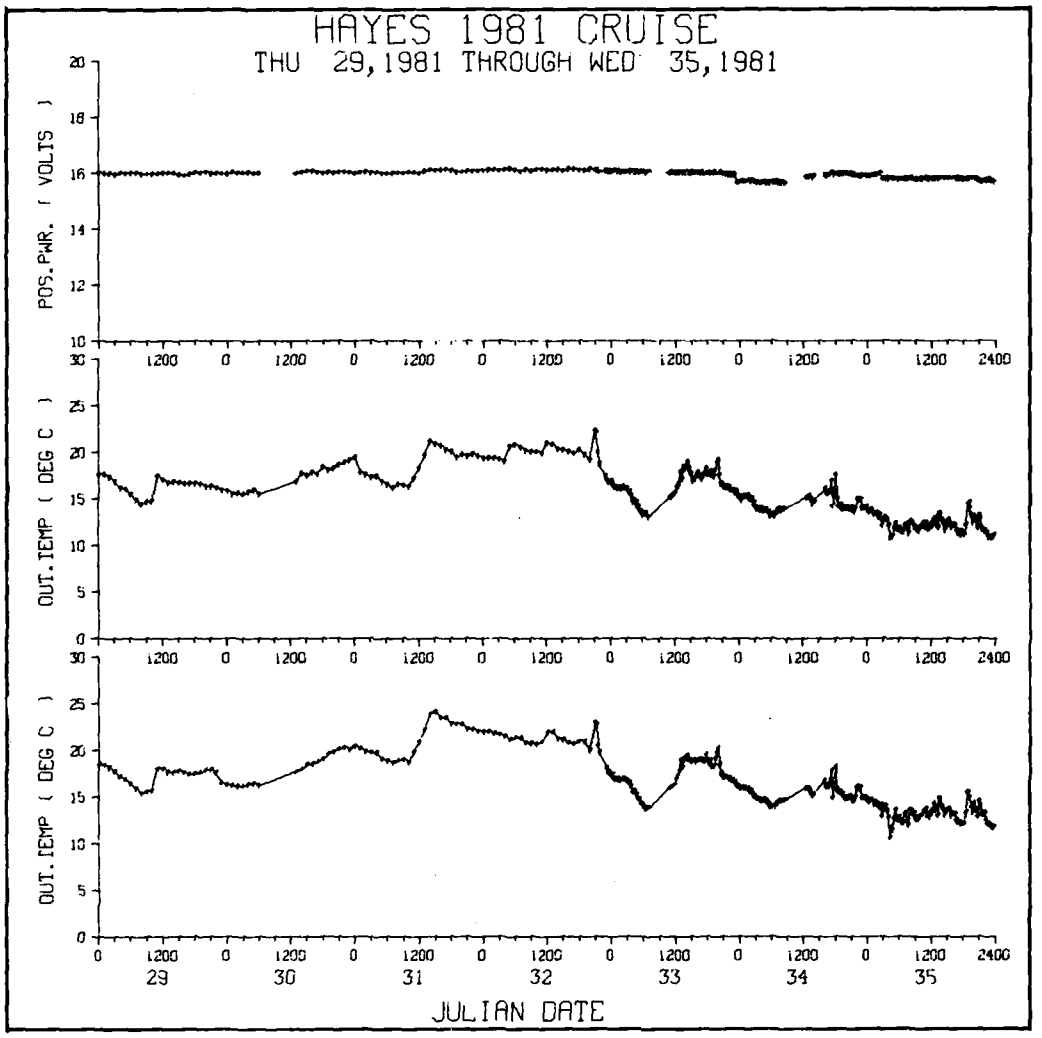

Fig. A-1 — Time series graph of EMS power supply voltage and ambient air temperature from JD 29 through JD 35, 1981. Middle temperature spectrum is from Fluke PRT while bottom temperature spectrum is from General Eastern PRT. Data gaps in the EMS occur at coincident discontinuities in the power supply voltage.

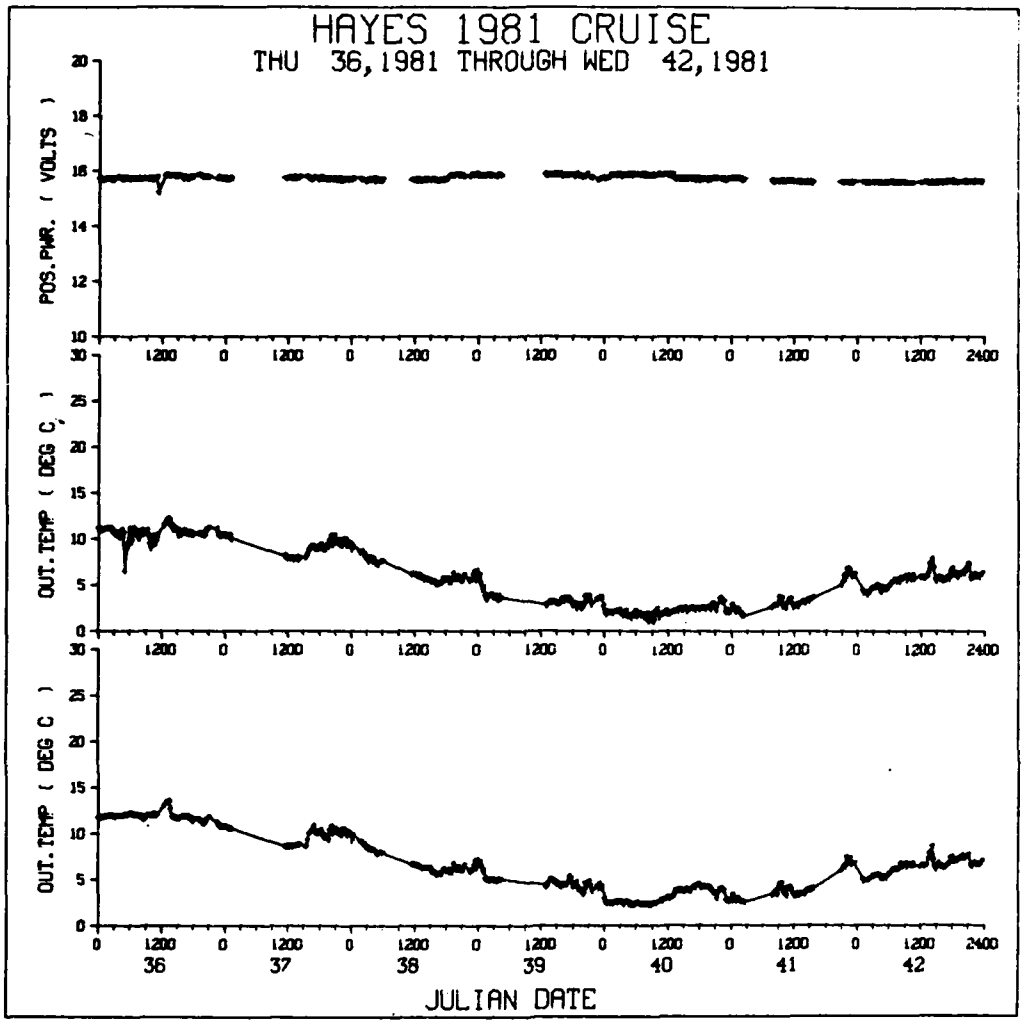

Fig. A-2 — Time series graph of EMS power supply voltage and ambient air temperature from JD 36 through JD 42, 1981.

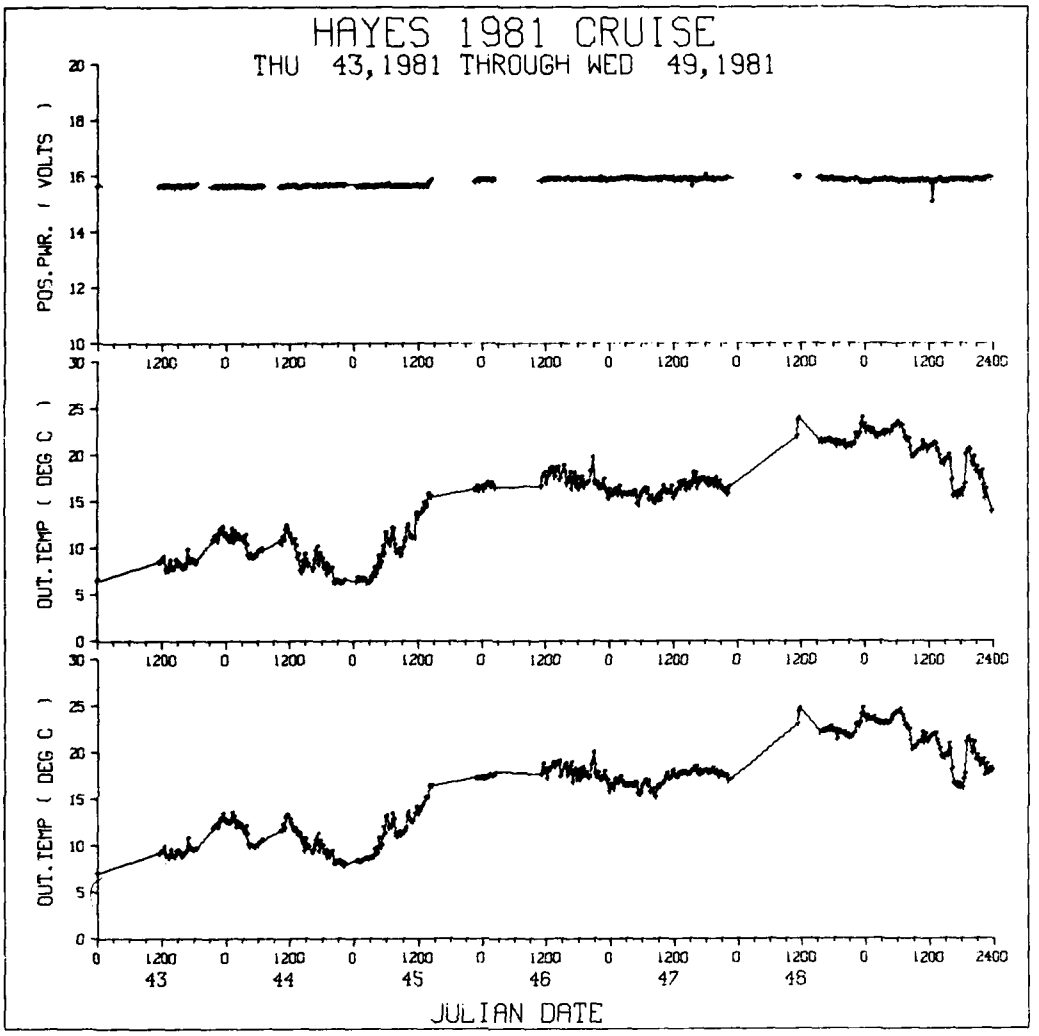

Fig. A-3 — Time series graph of EMS power supply voltage and ambient air temperature from JD 43 through JD 49, 1981.

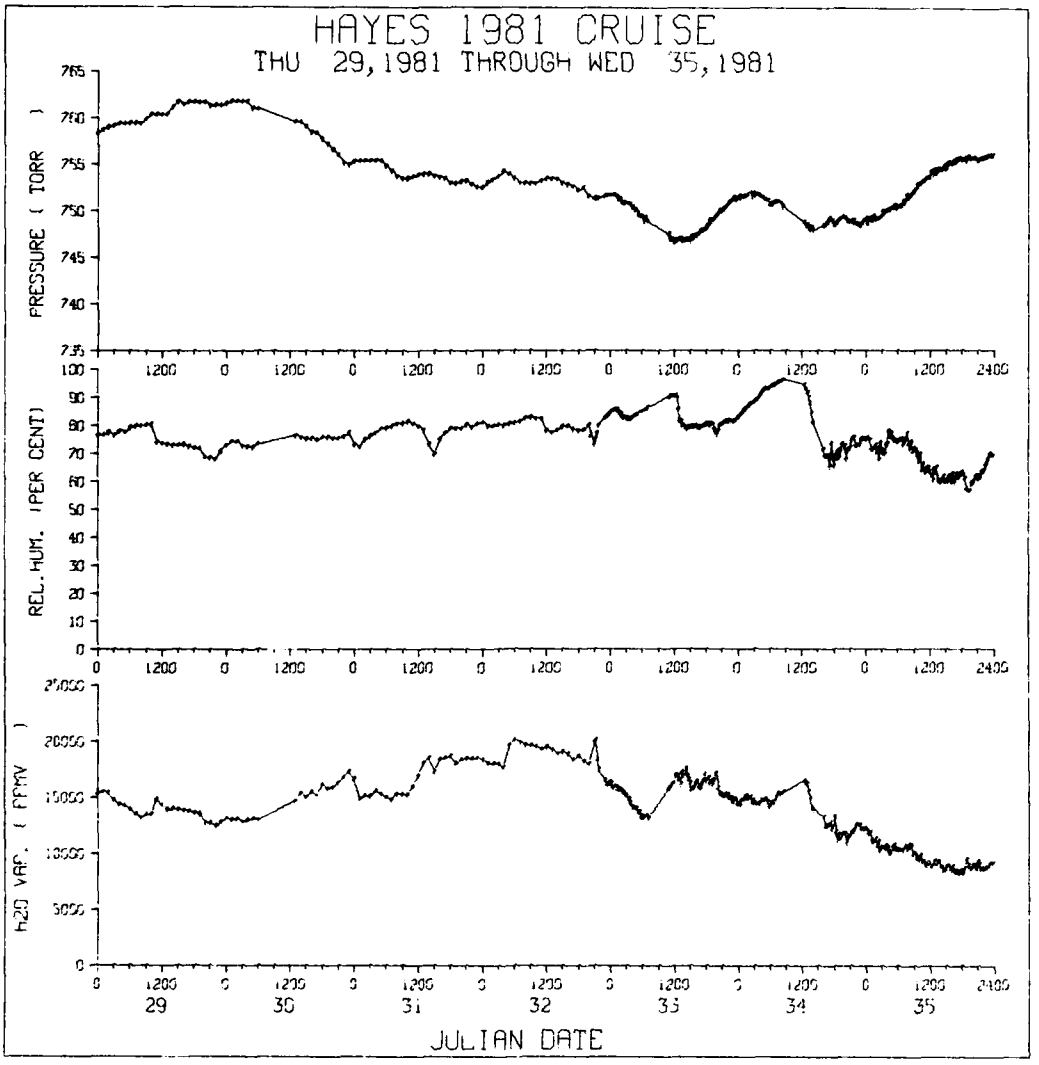

Fig. A-4 — Time series graph of barometric pressure, relative humidity, and atmospheric water vapor concentration from JD 29 through JD 35, 1981. Water vapor concentration was calculated according to McRae (1980).

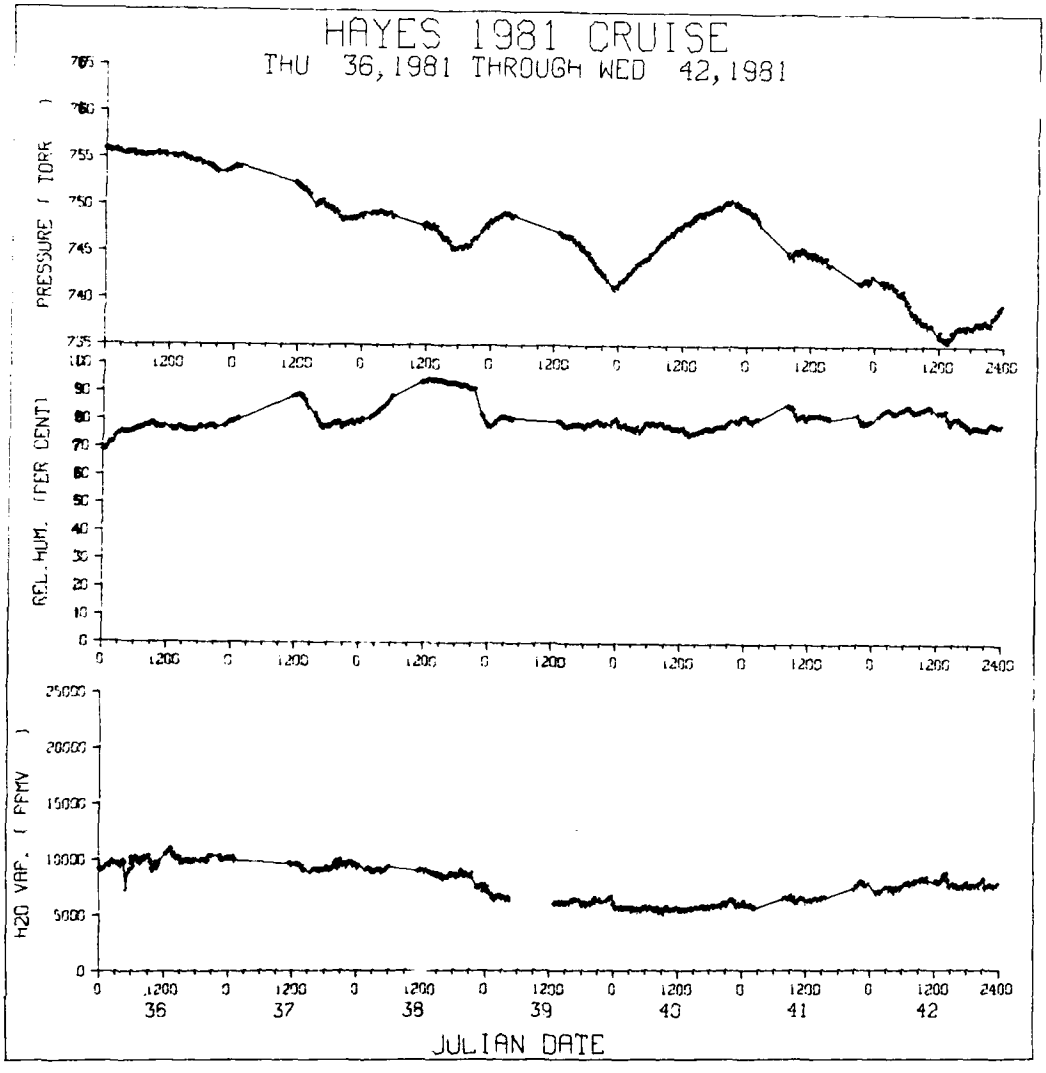

Fig. A-5 — Time series graph of barometric pressure, relative humidity, and atmospheric water vapor concentration from JD 36 through JD 42, 1981.

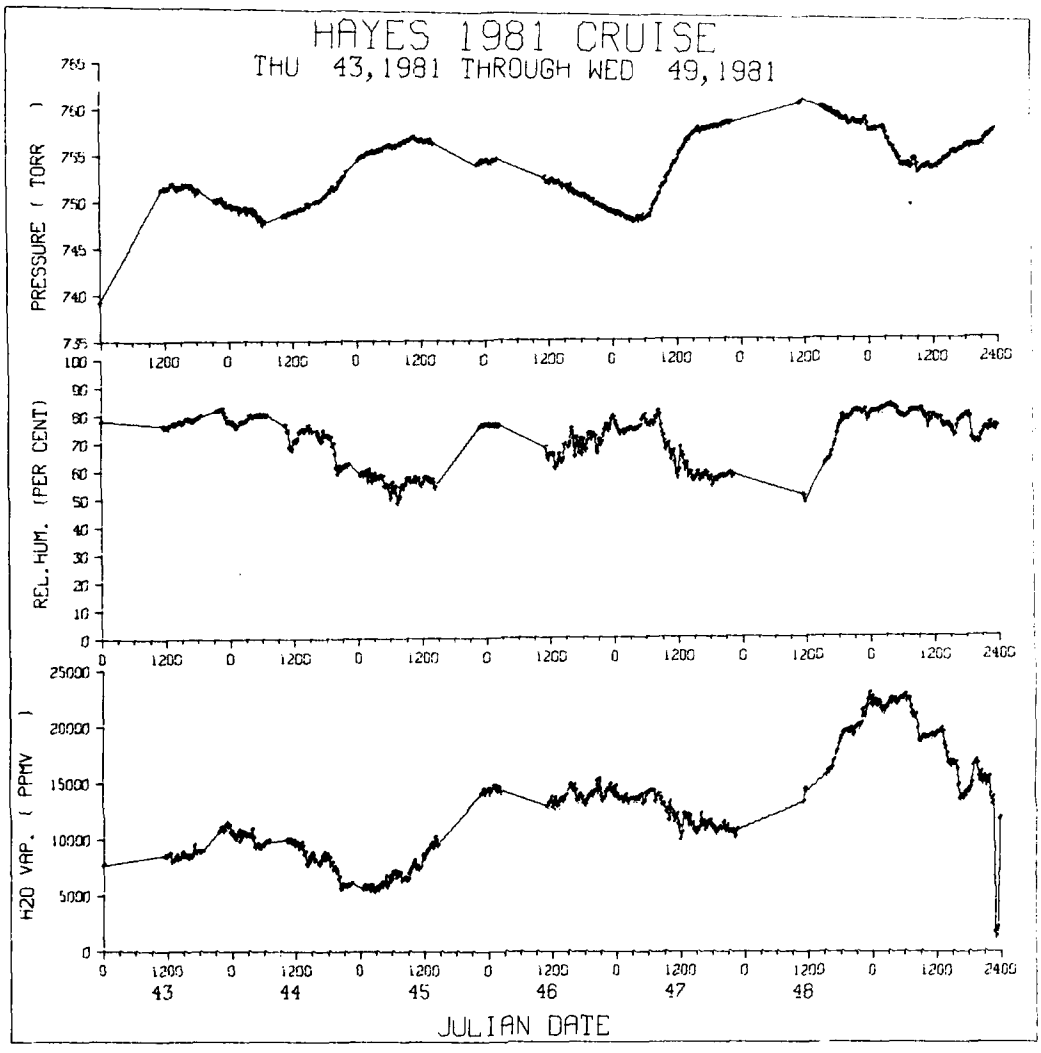

Fig. A-6 — Time series graph of barometric pressure, relative humidity, and atmospheric water vapor concentration from JD 43 through JD 49, 1981.

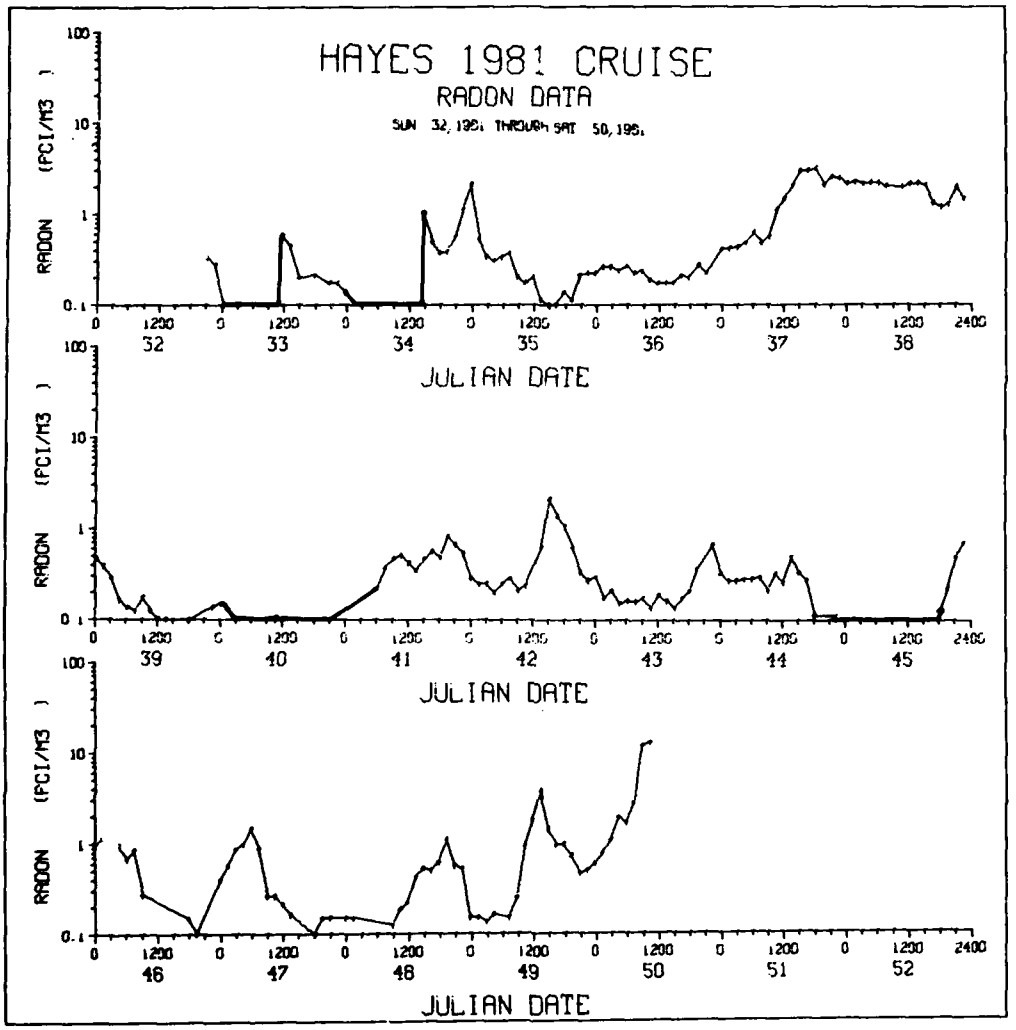

Fig. A-7 — Atmospheric radon concentration time series graphs from JD 32 through JD 50, 1981.

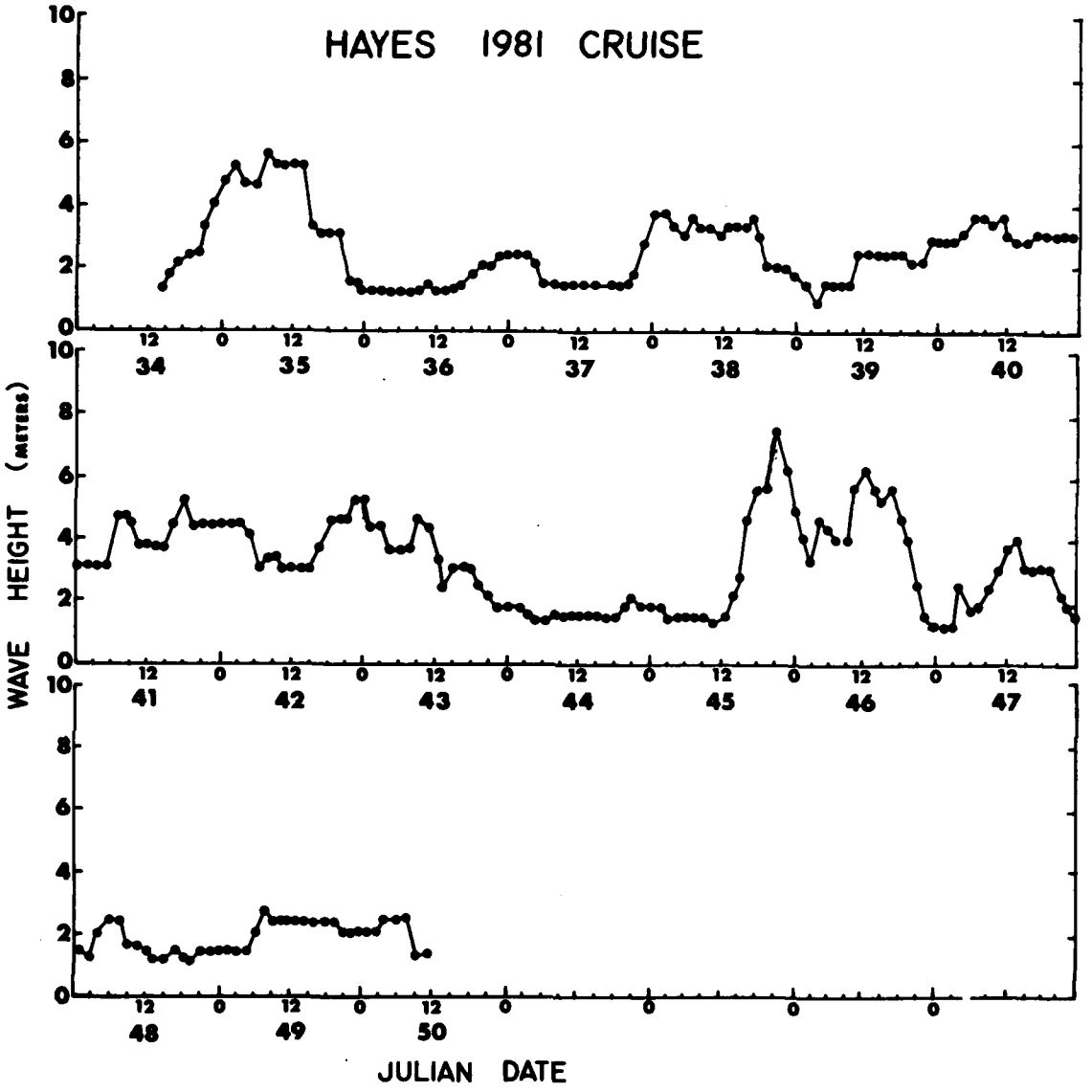

Fig. A-8 — Surface wave height time series from JD 32 through JD 50, 1981.